NUCLEAR MAGNETIC RESONANCE IN ISOPENTANE AT LOW TEMPERATURES

A Thesis

presented by

Alan G. Forsyth, B.Sc.,

to the

University of St. Andrews

in application for the Degree

of Master of Science.

DECLARATION

I hereby certify that this thesis has been composed by me, is a record of work done by me, and has not previously been presented for a Higher Degree.

The research was carried out in the Physical Laboratory of St. Salvator's College, in the University of St. Andrews, under the supervision of Dr. F. A. Rushworth.

CERTIFICATE

I certify that Alan G. Forsyth, B.Sc., has spent nine terms at research work in the Physical Laboratory of St. Salvator's College, University of St. Andrews, under my direction, that he has fulfilled the conditions of Ordinance No. 51 (St. Andrews) and that he is qualified to submit the accompanying thesis in application for the Degree of Master of Science.

Research Supervisor.

CAREER

I first matriculated in the University of St. Andrews in October 1953. I subsequently studied Chemistry and Natural Philosophy, and obtained the degree of Bachelor of Science in 1956. In 1958 I obtained post-graduate Second Class Honours in Natural Philosophy.

Following the award of a D.S.I.R. Research Studentship, I commenced in September 1958 the work reported in this thesis.

In October 1961 I was appointed to a Lectureship at the Heriot-Watt College, Edinburgh.

CONTENTS

CONTENTS

1. INTRODUCTION

1. Introduction

Nuclear Magnetic Resonance depends for its existence on the fact that most nuclei of the elements exhibit gyromagnetic properties. These properties were first attributed to the nucleus by Pauli (1924) to explain hyperfine structure in atomic spectroscopy.

When a sample containing nuclei exhibiting gyromagnetism is placed in a magnetic field, and is irradiated by an appropriate rotating radio-frequency magnetic field, the nuclei can be compelled to reveal their presence, identify themselves, and to describe the nature of their environments. Such experiments can, amongst other things, yield evidence of crystal and molecular structures, hindered molecular motions, and thermal relaxation mechanisms. This thesis is concerned with such effects.

Rabi, Millman, Kusch and Zacharias (1939) first applied the resonance method to individual atoms and molecules in atomic beam experiments, and produced transitions between the quantised nuclear magnetic energy levels by a process of absorption or stimulated emission.

Gorter had shown that this resonant exchange of energy should not be restricted to molecular beams, but should also be observed in matter in other forms in which intermolecular interactions would occur. Gorter (1936), and Gorter and Broer (1942) unsuccessfully attempted to detect energy absorption by ^{7}Li nuclei in Li F. It was later shown by Gorter (1951) that the failure was mainly due to the use of unfavourable materials.

The first successful experiments of nuclear magnetic resonance in

bulk material were made simultaneously and independently by Purcell, Torrey and Pound (1946), and Bloch, Hansen and Packard (1946). The development of the subject since these pioneer experiments has been such that applications have been found in many branches of physics and chemistry. Several companies now manufacture Nuclear Magnetic Resonance spectrometers, and these have achieved equality in importance with infra-red and mass spectrometers in many chemical research laboratories.

2. NUCLEAR MAGNETIC RESONANCE THEORY

2.1 General Theory

Classically, a nucleus with non-zero spin may be regarded as a rotating charged sphere, thus possessing angular momentum and an associated magnetic moment, as would a spinning bar magnet.

The classical theorem of Larmor showed, in effect, that a spinning bar magnet, free from any frictional forces, would, when placed in a magnetic field, precess like a top about the direction of the magnetic field. It was further shown that the frequency of precession was proportional to the magnetic field strength, and that the constant of proportionality was the ratio of the magnetic moment of the spinning bar magnet to its angular momentum. This constant is commonly known as the gyromagnetic ratio, γ. The Larmor theorem may then be written:

$$\omega = \gamma H \qquad (1)$$

where ω = 2π times the precession frequency, and H is the strength of the steady magnetic field.

This classical treatment may be extended to include the "frictional" effects which must exist in any assemblage of such nuclei. These forces will tend to reduce the angle of precession until the spinning magnet becomes aligned with the steady magnetic field. At the instant of alignment, the precession ceases, but at all times before this, regardless of the angle between the spinning magnet and the steady field, the frequency of precession will remain constant at the Larmor value. The time associated with realignment is known as the relaxation time. When

these frictional forces are large, the associated relaxation time will be short, and vice-versa.

A nuclear species whose spin number I is non-zero will possess an associated magnetic moment. It is known from quantum mechanical theory that the length of the angular momentum vector may only have the measurable values $m\hbar$, where $\hbar$ is Planck's constant divided by 2π, and where the magnetic quantum number, m, may take any of the $(2I + 1)$ values from $+I$ to $-I$. The maximum measurable component of angular momentum will thus be $I\hbar$. There will be a corresponding quantisation of components of magnetic moment; μ is taken as the maximum measurable component of magnetic moment, the relation to the corresponding value of angular momentum being $\mu = \gamma I\hbar$.

If such a system of spins is placed in a magnetic field, H_o, there are $(2I + 1)$ energy levels for each spin, spaced in energy by $\mu H_o/I$, or $g\mu_o H_o$, where μ_o is the nuclear magneton, and $g = \frac{\mu}{\mu_o}.I$ is the nuclear splitting factor corresponding to the Lande splitting factor of atomic spectroscopy.

The selection rules for transitions between these energy levels is that m may change by ± 1, corresponding to absorption or emission of energy. A quantum of energy may then produce transitions between the energy levels if it has the same magnitude as the level spacing; i.e. if

$$h\nu_o = \mu H_o/I \qquad (2)$$

where ν_o is the frequency of the applied radiation. Comparison with equation (1) shows that this is the same as the Larmor frequency.

For protons, $I = \frac{1}{2}$, and there are thus two energy levels separated by $2\mu H_o$, corresponding to alignment of the spins parallel or anti-parallel to the field. Equation (2) then becomes

$$h\nu_o = 2\mu H_o \qquad (3)$$

the fundamental resonance equation. For a field of 5260 gauss, a frequency of 22.4 Mc/s is required to produce transitions between the proton energy levels. The most popular commercial instrument at present operates at a frequency of 60 Mc/s, corresponding to a magnetic field of 14.1 kilogauss.

Theoretically the radiation should be circularly polarised, with the magnetic vector rotating in a plane perpendicular to the magnetic field. In practice a linearly oscillating field is used, since an oscillating vector may be shown to consist of two equal but oppositely rotating vectors, and we need only consider the one component effective in rotating about H_o in the same direction as the precessing magnetic moment - the counter rotating component having essentially no effect on the dynamics of the system.

Nuclei will return to the lower energy state by stimulated emission, and, since the absorption and emission probabilities are equal, there will only be a net absorption of energy from the field when there is continually a surplus of spins in the lower energy state. At any

temperature, in the absence of a radio-frequency field, it is assumed that the surplus is given by the Boltzmann distribution. In a steady field of 5000 gauss, the ratio of the number of protons in the lower energy state to the number in the higher energy state is given by $\exp(2\mu H_o/kT)$, an excess of four per million at room temperature. At liquid hydrogen temperatures this excess increases to sixty per million, which is a substantial increase.

Continued absorption will occur only if some mechanism exists to cool the effectively heated spins to the lattice temperature. So long as this mechanism maintains some difference between the populations, there will be a net absorption of energy. This mechanism is known as "spin-lattice relaxation", the efficiency of which is measured by the relaxation time, T_1. It can be shown (Andrew 1955) that n, the population difference at time t, and n_o, the equilibrium difference, are related by the equation

$$n = n_o \left(1 - \exp \frac{-t}{T_1}\right) \qquad (4)$$

The approach to equilibrium on removal of the stimulus is thus exponential.

Tight coupling between the spins allows rapid energy transfer from one spin to another, leading in some circumstances to the establishment of a thermal equilibrium within the nuclear spin system in a time much shorter than T_1, and at a temperature which may be quite different

from that of the lattice. This is called the spin-spin relaxation time, T_2.

There is a limit to the magnitude of the applied radio-frequency field, above which the relaxation process becomes less efficient. This is known as saturation, and may be thought of as arising when the nuclei are depolarised by the action of the radio-frequency field more rapidly than they can be repolarised by the relaxation process.

2.2 The Absorption Spectrum

The fundamental resonance equation applies only to an isolated nucleus, or to an assemblage of non-interacting nuclei. In practice, each nucleus in a sample of gas, liquid or solid experiences effects from neighbouring nuclei, each of which has a magnetic moment. There are thus created small internal magnetic fields in addition to the much larger external field, H_o. The field at a nucleus may then be written $H = H_o + H_{local}$, where H_{local} is the instantaneous field at that nucleus due to neighbouring nuclei. Only nearest neighbour nuclei are considered in computing this internal field, since the magnetic field of a dipole of moment μ, at a distance r, is μ/r^3. For $r = 1\text{Å}$, and μ = 1 nuclear magneton, μ/r^3 is approximately 5 gauss, the order of magnitude to be expected for H_{local}. This value decreases to 0.04 gauss when the separation is 5Å, and is a rapidly decreasing function of distance.

The resonance equation for a system of interacting protons may now

be written

$$h\nu_o = 2\mu(H_o + H_{local}) \qquad (5)$$

and the resonance spectrum is no longer a sharp peak, but broadened on either side of the fundamental frequency or field.

The value of H_{local} depends on both the molecular and crystal structure of the sample. It is thus possible, in theory, to calculate the absorption spectrum for a given proton configuration, but the calculation becomes extremely difficult for all but the simplest cases. Detailed perturbation calculations have been made for cases where the protons are in close groups of 2, 3 or 4. The spectrum of gypsum, $CaSO_4.2H_2O$, in which individual water molecules are well separated, was analysed by Pake (1948). The problems of three protons situated at the corners of an equilateral triangle, and of an isosceles triangle, have been treated by Andrew and Bersohn (1950) and Andrew and Finch (1957) respectively.

These calculations become more involved as the nuclear distributions become more complex, and an alternative approach must be made to relate the broadened absorption line to these distributions. Such an approach has been made by van Vleck (1948), who related the "second moment" of the absorption line-shape to the structure of the sample.

The second moment of the line-shape function is defined as the mean value of the square of the frequency deviation from the resonant frequency, the average being taken over the line-shape function. If

ν_o is the resonant frequency, the second moment is

$$\langle(\Delta\nu)^2\rangle_{av} = \int_{-\infty}^{+\infty} (\nu - \nu_o)^2 \quad g(\nu)\,d\nu \qquad (6)$$

The line-shape function, $g(\nu)$ is normalised, so that

$$\int g(\nu)\,d\nu = 1$$

and thus

$$\langle(\Delta\nu)^2\rangle_{av} = \frac{\int_{-\infty}^{+\infty} (\Delta\nu)^2\, g(\nu)\,d\nu}{\int_{-\infty}^{+\infty} g(\nu)\,d\nu}$$

$$= \frac{\left| g(\nu)\,\frac{(\Delta\nu)^3}{3}\right|_{-\infty}^{+\infty} - \frac{1}{3}\int_{-\infty}^{+\infty} (\Delta\nu)^3\,\frac{dg(\nu)}{d\nu}\,d\nu}{\int_{-\infty}^{+\infty} g(\nu)\,d\nu}$$

The line-shape function $g(\nu)$ is only appreciable when the frequency deviations is small, and so the first term may be neglected. Therefore

$$\langle(\Delta\nu)^2\rangle_{av} = \frac{-\frac{1}{3}\int_{-\infty}^{+\infty} (\Delta\nu)^3 \quad \frac{dg(\nu)}{d\nu}\,d\nu}{\int_{-\infty}^{+\infty} g(\nu)\,d\nu}$$

This may also be expressed in terms of magnetic field deviation if the magnetic field is varied rather than the radio frequency.

If $h = H - H_o$, the second moment may be written

$$\langle(\Delta H)^2\rangle_{av} = \frac{\frac{1}{3}\int h^3\,\frac{df(h)}{dh}\,dh}{\int h\,\frac{df(h)}{dh}\,dh} \qquad (7)$$

where $\langle(\Delta H)^2\rangle_{av} = \frac{\hbar^2}{g^2\mu_o^2}\,\langle(\Delta\nu)^2\rangle_{av}$, and $f(h)$ is the line-shape function expressed in terms of the magnetic field.

Van Vleck's theory gives for the rigid lattice second moment expressed in gauss^2

$$S^2 = \frac{3}{2}\frac{I(I+1)}{N_r} g^2 \mu_o^2 \sum_{j>k} (3\cos^2\Theta_{jk} - 1)^2 r_{jk}^{-6} + \frac{1}{3}\frac{\mu_o^2}{Nr} \sum_j \sum_f I_f (I_f + 1) g_f^2 (3\cos^2\Theta_{jf} - 1)^2 r_{jf}^{-6} \quad (8)$$

where

g, I are the nuclear g-factor and spin of the nucleus at resonance

g_f I_f are the nuclear g-factors and spins of the other nuclear species present in the sample.

r_{jk} is the length of the vector connecting nuclei j and k,

Nr is the number of nuclei at resonance which are present in the system whose interactions are considered, and over which the sum is taken.

The factor $(3\cos^2\theta - 1)^2$ must be averaged over a sphere for a polycrystalline sample. In this thesis, only one species of nucleus at resonance, the proton, is considered. Thus equation (8) becomes

$$S^2 = \frac{6}{5}\frac{I(I+1)}{Nr} g^2 \mu_o^2 \sum_{j>k} r_{jk}^{-6} \quad \text{gauss}^2$$

Inserting the values given by Bearden and Watts (1951), we find for a rigid lattice

$$S^2 = \frac{715.9}{N} \sum_{j>k} r_{jk}^{-6} \quad \text{gauss}^2 \quad (9)$$

This rigid-lattice value for the second moment will be modified should any change take place in the nuclear arrangement within the sample. Any form of molecular motion, such as rotation, rotational oscillation and quantum mechanical tunnelling will reduce the second moment calculated from Van Vleck's formula, provided the motion takes place at a high enough frequency (Gutowsky and Pake, 1950). The factor $(3\cos^2\theta - 1)^2 / r^6$ occurring in Van Vleck's formula must then be replaced by its mean value over the particular motion taking place.

For classical rotation, or n-fold tunnelling ($n \geqslant 3$) about a symmetry axis of the molecule, each term in the Van Vleck formula is multiplied by the factor

$$p = \frac{1}{4} (3 \cos^2 \gamma_{jk} - 1)^2 \qquad (10)$$

where γ_{jk} is the angle between the internuclear vector joining nuclei j and k, and the axis of rotation. p decreases from unity ($\gamma_{jk} = 0$) to zero ($\gamma_{jk} = 54°44^1$) and increases again to $\frac{1}{4}$ ($\gamma_{jk} = 90°$).

The most common form of molecular motion found in paraffins is rotation of one or more of the constituent methyl groups about the C-C axis. The contribution to the second moment from the interactions of the protons of each methyl group amongst themselves is reduced by a factor of four (equation 10), since the interproton axes are perpendicular to the axis of rotation. The effect of the methyl group rotation on the field at other nuclei in the molecule is calculated in a manner similar to that for the

reduction of the intermolecular second moment of cyclohexane (Andrew - Eades 1953b).

This theory has been proved successful by many authors to correlate molecular motions with reductions in the second moment.

2.3 The Relaxation Process

Of the two competing processes within a sample during a nuclear magnetic resonance experiment - the relaxation tending to establish the Boltzmann inequalities between the energy-level populations and the driving electromagnetic field which tends to destroy them - the former must be dominant if there is to be a steady absorption of energy from the radio-frequency field.

Equation (4) for the difference in population must be amended to account for the transitions due to such absorption of radio-frequency energy. Bloembergen, Purcell and Pound (1948) considered the probabilities of transitions under these circumstances, and the population difference equation is shown to be

$$\frac{n_s}{n_o} = \frac{1}{1 + \frac{1}{2}\gamma^2 H_1^2 T_1 g(\nu)} \qquad (11)$$

where n_s is the steady state value of population difference

H_1 is the radio-frequency field amplitude

$g(\nu)$ is the normalised line-shape function.

Since the line-shape function, $g(\nu)$, is normalised, its peak value will give an inverse measure of its width. The spin-spin relaxation time is defined by the relation

$$T_2 = \frac{1}{2} g(\nu)_{max.}$$

Equation (11) may then be written

$$\frac{n_s}{n_o} = \frac{1}{1 + \gamma^2 H_1^2 T_1 T_2} = Z_o \qquad (12)$$

where Z_o is known as the saturation factor.

The ratio n_s/n_o is dependent on the value of the radio-frequency field. With increasing field the absorption decreases, and the specimen is saturated. When the frequency is such that $g(\nu)$ is a maximum, the saturation is a maximum. The maximum steady-state absorption is obtained when the amplitude of the radio-frequency field is such that $\gamma^2 H_1^2 T_1 T_2 \ll 1$. This saturation effect may be employed to measure T_1, and will be discussed later.

The large nuclear concentrations and small inter-nuclear distances existing in bulk matter give rise to strong spin interactions. The effectiveness of these interactions is considerably reduced in liquids by the rapid relative motions of the nuclei. This is also the case for solids in which molecular reorientation, or other motions are taking place.

Bloembergen, Purcell and Pound showed that such motion was effective in producing spin-lattice relaxation. The rapidly fluctuating fields created have components which will cause these transitions between energy levels.

Rollin and Hatton (1948), and Bloembergen (1949) suggested that the ever-present, tiny concentrations of paramagnetic impurities actually controlled the relaxation process. The spin energy is transferred to the lattice by means of the large electronic magnetic moment of the paramagnetic ion. This process gives relaxation times in agreement with experiment.

3. EXPERIMENTAL METHODS AND APPARATUS

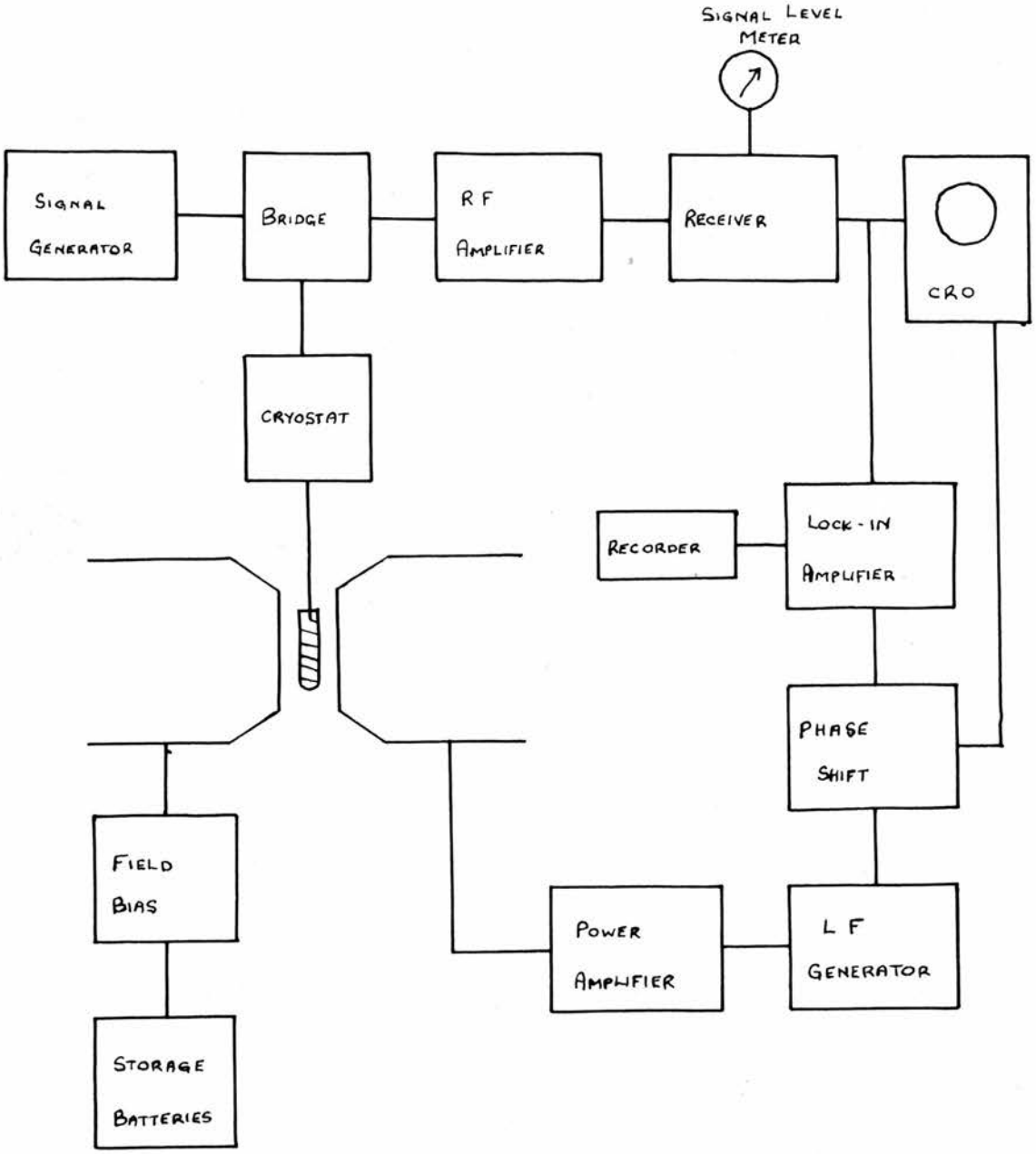
SIGNAL LEVEL METER
SIGNAL GENERATOR
BRIDGE
RF AMPLIFIER
RECEIVER
CRO
CRYOSTAT
RECORDER
LOCK-IN AMPLIFIER
PHASE SHIFT
FIELD BIAS
POWER AMPLIFIER
L F GENERATOR
STORAGE BATTERIES

FIG. 1.

3.1 Basic Requirements

The conditions for the detection of nuclear magnetic resonance require that the sample be placed in a magnetic field H_o, and be supplied with radio-frequency energy at a frequency ν_o at right angles to the magnetic field. For protons ν_o and H_o are then related by the resonance expression $h\nu_o = 2\mu H_o$.

An arbitrary choice of frequency and field cannot be made, however. The signal obtained is very low, comparable with that of the ever present thermal and valve noise. It is necessary then to choose conditions whereby a maximum signal to noise ratio is obtained. Bloembergen, Purcell and Pound have shown that the ratio of the nuclear signal to R.M.S. noise fluctuations is proportional to $\nu_o^{7/4}$. A higher field, H_o, both increases the spacing between the levels $2\mu H_o$, and the population ratio due to the Boltzmann factor $\exp(2\mu H_o/kT)$. It is therefore advantageous to use as high a radio-frequency as is practicable, taking into consideration the difficulty in designing the appropriate radio-frequency circuits. The resonant conditions used for the experiments reported here were $\nu_o = 22.4$ Mc/s corresponding to the magnetic field strength of 5260 gauss, the permanent magnet field, H_o.

The bridge method for detecting nuclear magnetic resonance absorption used here is based on that of Bloembergen(1948) and is shown schematically in Fig. 1. The sample is held in a coil at right angles to the permanent magnet field. Quanta of radiation are supplied at the resonant frequency

by the signal generator. The absorption of energy is detected as an additional power loss, or increase in resistance of the coil. In order to display the resonance more clearly, the main magnetic field is modulated at a low frequency by means of auxiliary coils. The main field, H_o is swept through the resonant value twice each cycle giving an audio-frequency modulation of the carrier. The depth of signal modulation on the carrier is small, however, and a radio-frequency bridge is employed. This serves to balance out most of the carrier signal and noise, and effectively increases the degree of modulation due to absorption. The output from the receiver is applied to the Y plates of the C.R.O., the X plates being supplied with the low-frequency signal, phased correctly with respect to the field modulation. The absorption curve traced is then shown as a function of the magnetic field, H_o.

It is not possible, in general, to display the broad lines from solid samples. Here the signal strength is often comparable with the noise fluctuations, and the sensitivity of the apparatus must be increased. Any change in sample coil balance due to heating or microphonics changes the d.c. level at the output of the radio-frequency detector. By passing the output from the receiver through an audio amplifier and into an audio phase-sensitive detector, or "lock-in" amplifier, one discriminates against these d.c. level changes, and detects only the audio-modulated signal components.

When using the "lock-in" amplifier, the field modulation is reduced to a fraction of the line-width, and the main field is swept slowly through

resonance. The output from the phase-sensitive detector is proportional to the first derivative of the absorption line, and is displayed on a recording meter.

3.2 Description of Apparatus

Some sections of the apparatus will now be described in detail in order to emphasise the more important requirements.

(1) Permanent Magnet

In the past decade a considerable amount of research has gone into the production of magnets of high stability and homogeneity. This has resulted in the use of electromagnets in most of the commercially available nuclear magnetic resonance spectrometers. The permanent magnet has, however, the advantages of stability and convenience for the work reported here, and was designed by Andrew and Rushworth (1952) and described fully by Rushworth (1953). The specifications are: Field strength: 5260 gauss. Pole-face diameter: 8". Gap width: 2". Specially designed ring-shims are employed to increase the field homogeneity.

The original magnetising coils are used to sweep the steady field. Current for this is supplied from storage batteries, and controlled by a motor driven potentiometer.

(2) Signal Generator

An Airmec Signal Generator, Type 701, is used, giving an output of from 10μV to 1V. Power is supplied from a well-smoothed Solartron H.T.

Unit (AS 517), and the valves are heated by an Advance (D C 2) 6V D.C. unit. These units serve to eliminate spurious 50 c/s modulation effects.

The Signal Generator was replaced during the experiments by a more modern instrument, Airmec Type 201, whose specification is similar to that of the Type 701. External power supplies are again employed here.

(3) Radio-Frequency Bridge

The twin-T bridge used here is similar to that described by Anderson (1949). Circuit analysis of this bridge shows that the controls for resistive and reactive balance are independent. The two conditions of balance may thus be reached by adjustment of the appropriate condenser. This method enables both absorption and dispersion curves to be plotted. If the bridge is balanced in phase, and partially unbalanced in amplitude, the absorption curve is obtained, if balanced in amplitude but not in phase, the dispersion curve is obtained. Incorrect adjustment of the bridge will then give a combination of the two curves, resulting in a distortion of the required absorption curve. Due to its asymmetry, the bridge is critically dependent on frequency, and frequency modulation of the signal generator output must be eliminated.

In practice the bridge is balanced in amplitude so that the carrier level is reduced to less than 1% of the level being fed into the bridge (generally a 30 db balance).

(4) Radio-Frequency Amplifier

An Eddystone Communications Receiver, Type 680S, is used to provide

most of the radio-frequency amplification together with demodulation and audio amplification. The instrument was returned to the makers for modification to give maximum sensitivity at the operating frequency. Power is again supplied by external Solartron and Advance units. Indication of carrier level is given by a milliammeter connected in the second detector stage.

The receiver was preceded by a pre-amplifier, in order to give the optimum signal to noise ratio when using the very low radio-frequency voltages necessary to avoid saturation of the sample.

The main pre-amplifier is a single stage unit employing a Mullard EF 54 pentode. Balanced input and output tuned circuits are used, being inductively coupled to the co-axial feeders. This circuit has been described by Eades (1952), and the method of measurements of the noise-factor using a noise-diode has been described by Lawrenson (1958). The noise factor for this pre-amplifier is 2.5 db.

A second pre-amplifier has been constructed by Hoch (1963). When used in conjunction with the first pre-amplifier, the noise factor is 1.5 db.

(5) The Narrow-Band Lock-in Amplifier

In general, operation of these circuits depends on combining the signal-plus-noise voltage vectorially with a reference voltage of the desired frequency, and rectifying the combination voltage in such a way

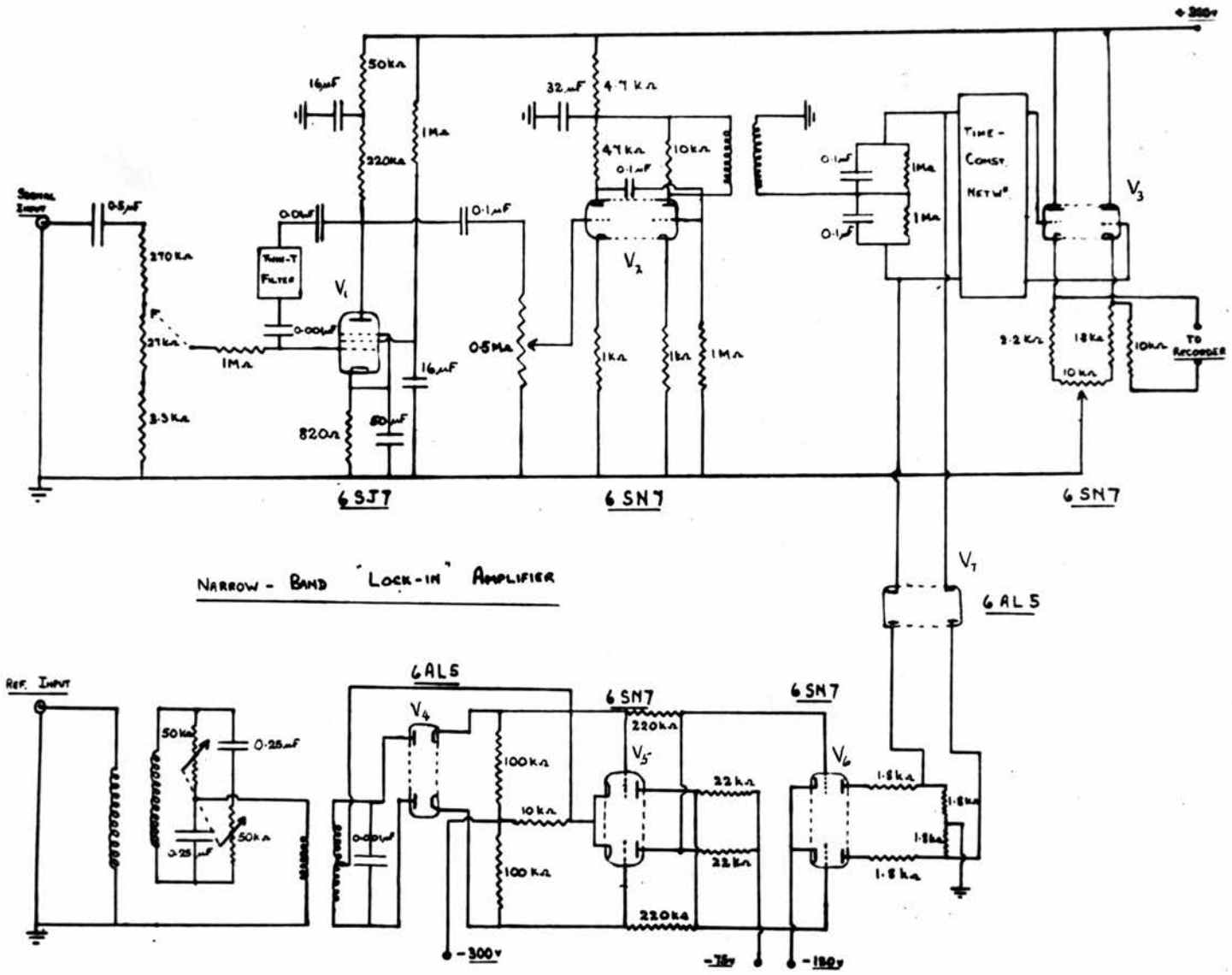
+ 300v
Signal Input
0·5μF
270 kΩ
27 kΩ
3·3 kΩ
1MΩ
50kΩ
1MΩ
220kΩ
16μF
0·001μF
0·1μF
Twin-T Filter
V1
0·001μF
16μF
820Ω
50μF
0·5MΩ
6SJ7
32μF
4·7 kΩ
4·7kΩ
10kΩ
0·1μF
V2
1kΩ
1kΩ
1MΩ
6SN7
0·1μF
1MΩ
0·1μF
1MΩ
Time-Const. Netw.
V3
3·2 kΩ
1·8kΩ
10kΩ
10kΩ
To Recorder
6SN7
NARROW - BAND "LOCK-IN" AMPLIFIER
V7
6AL5
Ref. Input
50kΩ
0·25μF
0·25μF
50kΩ
6AL5
V4
0·001μF
100kΩ
10kΩ
100kΩ
6SN7
220kΩ
V5
22kΩ
22kΩ
220kΩ
6SN7
V6
1·8kΩ
1·8kΩ
1·8kΩ
1·8kΩ
-300v
-75v
-150v

FIG. 2.

that the noise components are cancelled over a period of time long compared with the period of the reference voltage. In such a way one obtains the performance of a very narrow band amplifier without the problems of drifting and detuning which may occur with a conventional amplifier of such narrow band-width.

In practice, several difficulties in the operation of such devices have been found. The output from the lock-in amplifier is not steady, but varies with input noise level, reference voltage amplitude, and variations in valve parameters. These faults were found in the original 25 c/s amplifier based on the circuit described by Bloembergen (1948). In an effort to eliminate these zero-drifts, a second circuit was constructed following the design of Cox (1953).

A sinusoidal reference voltage, derived from the AF generator, drives a square-wave generator, the output from which is applied to the anodes of a double diode. The signal input is applied to the cathodes of this valve, and the d.c. voltage developed between the cathodes is measured by a form of valve-voltmeter. This dc output voltage is directly proportional to the signal voltage, and is to a large extent independent of the general noise level at the input, the reference voltage amplitude, and the valve parameters.

In the circuit shown in Fig. 2, valves V_3, V_4 and V_5 with their associated circuits constitute the square-wave generators. The sinusoidal reference voltage is applied through the coupling twin diode,

V_4, to a conventional Eccles-Jordan "flip-flop" circuit associated with V_5. V_6 is provided in order to obtain an output voltage negative with respect to ground. In a flip-flop circuit, there is a small voltage drop across the anode load resistance of the non-conducting triode section due to the coupling and grid-resistors. The cathodes of V_6 are therefore made slightly negative with respect to the anode supply of the flip-flop valve. Since the output voltage from each terminal of the square-wave generator is used only to cut off the associated diode of V_7, it is not necessary for the two output voltages to be equal. V_7 is the double-diode mentioned earlier, and V_3 and its associated circuit constitute the valve-voltmeter. In this circuit is incorporated a selection of filters whose time constants may be varied from 0.5 to 8 seconds.

Since the output of a lock-in amplifier depends on the phase angle between the reference voltage and the signal voltage, a phase-shifter is incorporated in the reference voltage input, before V_4.

Valves V_1 and V_2 form the narrow-band amplifier circuit, incorporating a twin-T rejector circuit.

A higher modulation frequency (285 c/s) was chosen for use in conjunction with this instrument, as the signal to noise ratio is then slightly improved (Pound and Knight, 1950). This frequency was reduced to 76 c/s when it was found that mechanical vibration of the modulation coils was being transmitted to the cryostat, and thus causing instability in the output from the lock-in amplifier.

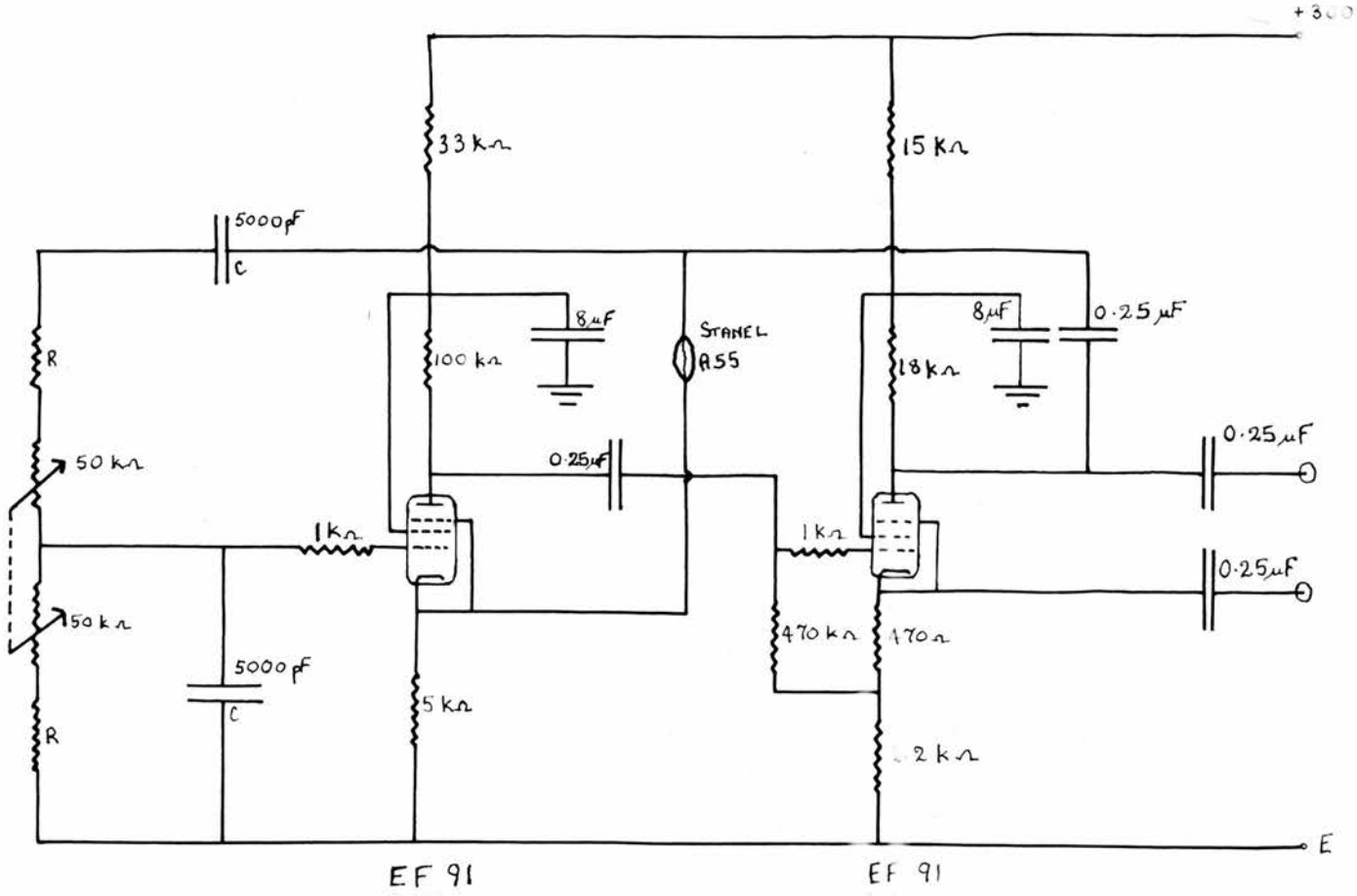

Fig. 3. AF Generator.

$$f = \frac{1}{2\pi RC}$$

(6) Field Modulation Equipment

The original (25 c/s) generator is based on the design of Bloembergen (1948), and has been described by Eades (1952).

A second generator was constructed for use with the Cox lock-in amplifier. It is a Wien bridge oscillator, employing two EF 91 valves, and stabilised by means of a thermistor. The circuit diagram is shown in Fig. 3. Circuit analysis shows that the generator frequency is given by $f = 1/2\pi RC$. As with the narrow-band amplifier, the value of C is chosen to be 5000 pf, and the value of R may be calculated once the frequency of operation has been chosen. The frequency may be varied over a small range by means of the 50 kΩ ganged potentiometer. For a major change in frequency only the two resistances R need be changed.

Besides supplying the drive voltage for the field modulating equipment, the generator supplies the low-frequency voltage necessary for the mixer stage of the lock-in amplifier.

The field modulation equipment consists of a power amplifier capable of delivering 15 watts at 25 c/s into the field modulation coils. The circuit impedance increases with increasing modulation frequency and maximum output from the power amplifier gives a peak to peak modulation amplitude at 285 c/s of 4.25 gauss. The corresponding value at 76 c/s is 9 gauss.

The oscilloscope sweep voltage is also obtained from the secondary winding of the power amplifier output transformer, using a suitable phase-

Fig. 4.

shifting network.

Calibrations of the modulation coils and the field-shift were made.

(7) Field Shift Calibration

The current through the field coils is measured by a millivoltmeter connected across a standard 0.2 Ω resistance in the circuit. With no current in the field coils, a liquid line is accurately centred on the C.R.O. screen by altering the signal generator frequency. This frequency is then accurately measured with the aid of a heterodyne frequency meter, Type BC 221. This procedure is repeated for several values of current through the field coils giving fields greater or less than the permanent magnet H_o. The frequency shift for unit millivoltmeter reading may then be calculated by inserting the known values into the equation $h\nu_o = 2\mu H$.

The method of least squares gave a value of 0.442 gauss/mV for the field shift.

(8) Calibration of Modulation Coils

A similar procedure is used to calibrate the modulation coils. When a sinusoidal voltage is applied to the coils and also to the X-input of the C.R.O., the trace is a linear variation of field. The liquid line is observed at various positions along the X-sweep for different values of modulation current. The frequency difference is again converted into values of magnetic field, and the amplitude of the modulation is then given in terms of the current flowing in the coils.

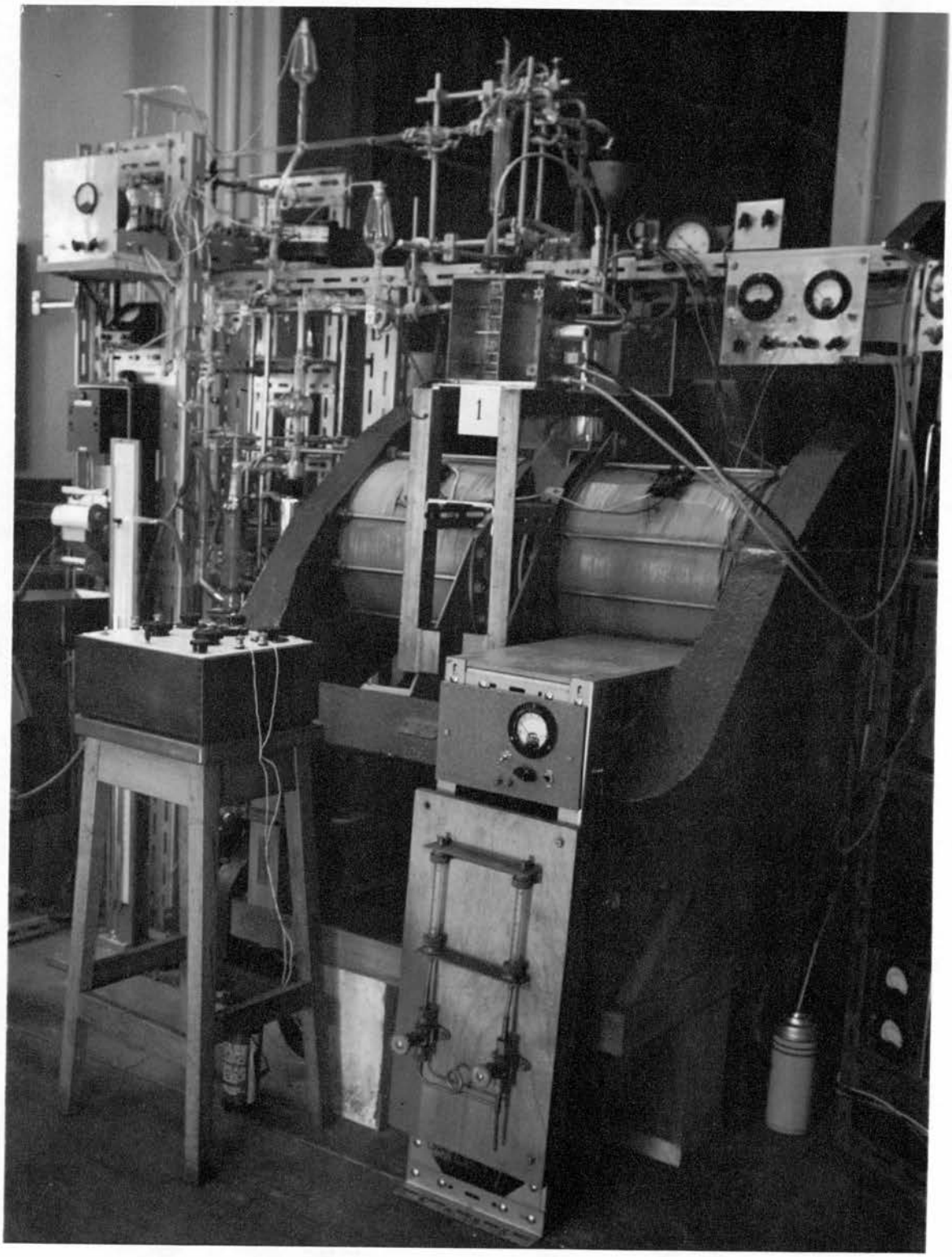

FIG. 5.

In figures 4 and 5 are shown most of the electronic equipment. The numbered units are as follows:

1. Twin-T bridge and cascode pre-amplifier unit.
2. Main pre-amplifier.
3. A.F. cathode follower matching unit.
4. Phasing and transforming unit supplying X-sweep for C.R.O.
5. A.F. generator.
6. Lock-in amplifier.

Above and below unit 3. are the signal generator and receiver respectively. The other electronic units seen are the various power supplies.

3.3 The Cooling System

A cryostat suitable for use down to liquid hydrogen temperatures was designed and constructed. It is drawn schematically in Fig. 6 and photographed in Fig. 7.

The specimen to be examined is sealed in a thin-walled Pyrex tube (1) of diameter 6 mm., supported in the coil. A typical coil consists of 14 turns of 18 swg copper wire, leads of 1 mm diameter copper nickel alloy capillary tubing (2) support the coil, and connect it electrically to the main coaxial conductor. This consists of a 28 swg copper wire (3) leading down the axis of a 6 mm thin-walled copper nickel tube (4) supported at the top by a Kovar seal (5) and soldered at the bottom to a short length of screwed wire passing through a perspex bush. The

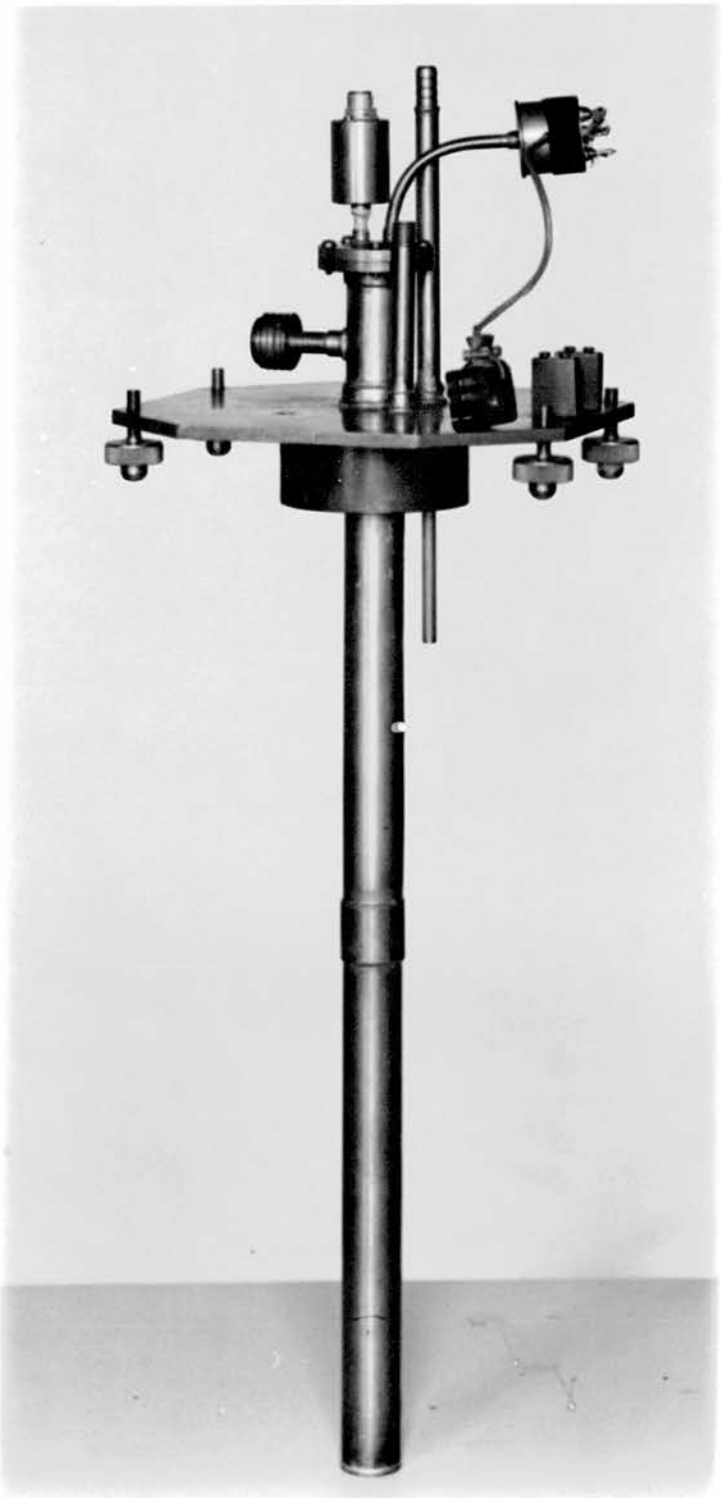

Fig. 7.

copper wire is connected at the top to a coaxial socket (6), leading to the twin-T bridge by a length of 75 ohm coaxial cable.

This unit fits into an outer tube of 25 mm diameter copper nickel alloy (7), made from the sheet metal. This tube is sealed at the lower end, and the assembly rendered vacuum tight at the upper end by means of an O-ring seal. The whole assembly is fixed to a rigid brass plate (8), mounted above the magnet, and supported by four levelling screws to ensure accurate alignment of the sample in the median plane of the magnet gap. Tubes also pass through the base-plate enabling the dewar to be pumped (9), and to permit the entrance of transfer-tubes (10). A wide tube above the base plate (11) leads to the vacuum system which consists of a rotary pump, mercury diffusion pump and Pirani gauge.

Heaters are wound non-inductively on each end of the specimen tube, each consisting of 50 turns of 34 swg Eureka wire, connected to storage batteries. Between each heater and the coil is attached a copper-constantan thermocouple. The leads from the heaters and thermocouples are tied with thread along the outside of the coaxial tube, and pass to the connecting box (12) through a curved 6 mm tube in the top-plate.

The Dewar containing the refrigerant is specially shaped, being narrow at the bottom to fit the magnet gap. It has a capacity of one litre, and is filled by transfer from the storage vessel under slight pressure.

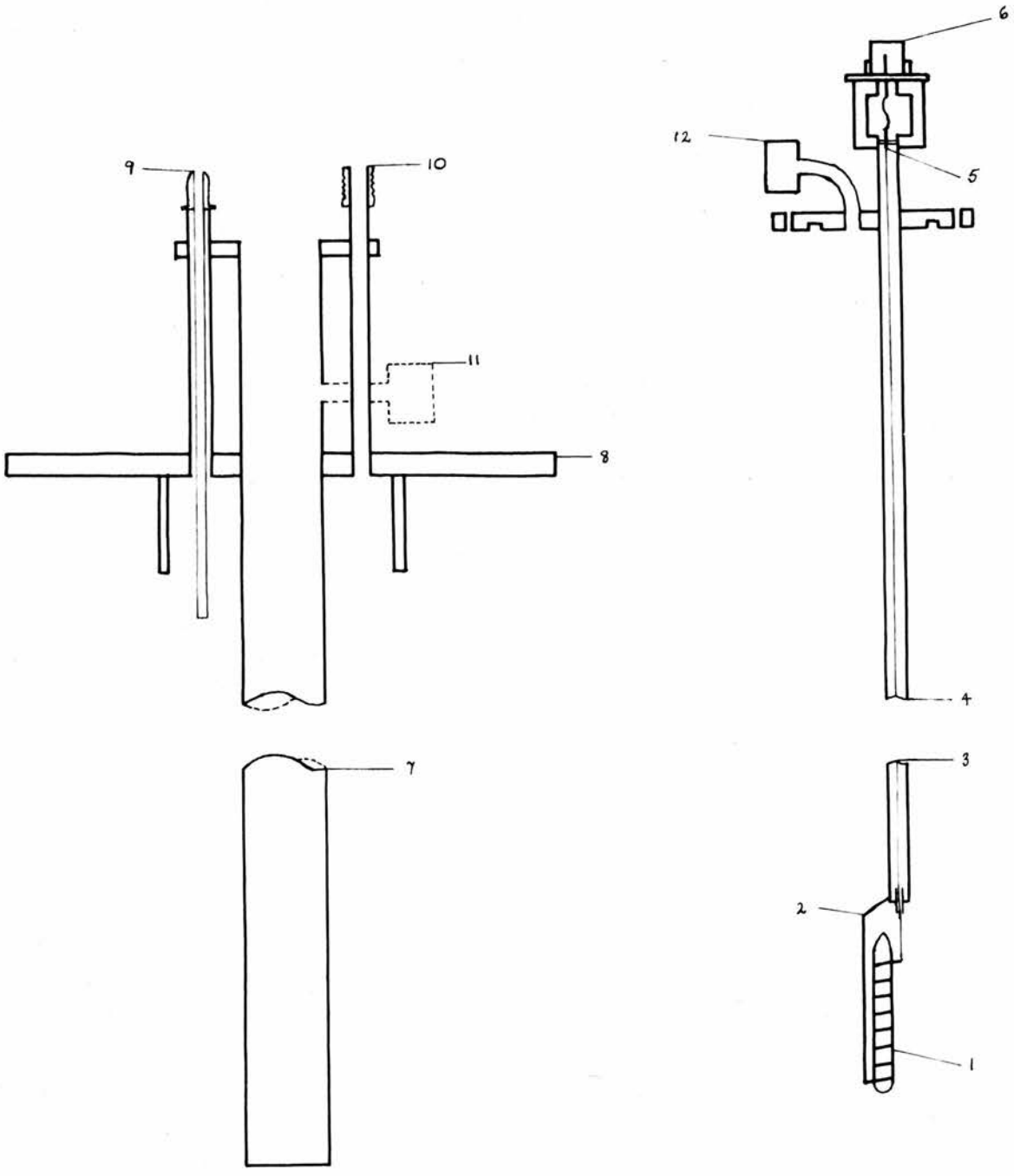

FIG. 6.

The Dewar is precooled with liquid nitrogen when using liquid hydrogen as the refrigerant. When the cryostat is filled with hydrogen at a pressure less than atmospheric, thermal contact exists between the specimen and the bath. The specimen readily attains the temperature of the bath. The temperature of the specimen may be raised above that of the bath by evacuating the cryostat and varying the heater current. The equilibrium temperatures are sensibly constant over long periods of time.

It is possible to maintain a temperature difference in excess of 100°K between the sample and liquid hydrogen bath. With such a large heat input, the rate of evaporation of liquid hydrogen is of the order of one litre per hour. However, with the more usual, lower, heater currents employed, the evaporation rate is reduced to five hundred ccs. per hour, which is considered most satisfactory for a single Dewar system.

Temperature measurements are accurate to 1°, except at the lowest temperatures where the thermoelectric voltage developed varies less rapidly with temperature.

4. EXPERIMENTAL PROGRAMME AND RESULTS

4.1 Experimental Programme

It has been stated earlier that nuclear magnetic resonance methods can be used to yield information concerning molecular motions in solids. Substances containing protons are most suitable for such investigations, since the high gyromagnetic ratio of the proton ensures a relatively good signal to noise ratio. Hydrocarbons are especially suitable, since they have a high proton concentration, and the ^{12}C nucleus has a zero spin. In addition to the absorption line shape studies, spin-lattice relaxation time measurements yield further information concerning reorientation frequencies and the potential barriers hindering the reorientation process.

Investigations of crystal structures by means of X-rays normally indicate the positions of the carbon atoms, and the proton positions are a matter for conjecture. The local magnetic field governs the width of the nuclear magnetic resonance absorption line, however, and this magnetic field may be estimated from a theoretical consideration of the molecular structure. Measurement of the second moment may then verify the postulated positions of the protons in the chosen sample. Relatively low frequency motion reduces the width of the absorption spectrum. Such motion is evident in neutron and X-ray experiments only when the mean rate of motion is of the order of the incident frequency, say 10^{18} c/s.

The choice of subjects for study by nuclear magnetic resonance methods

is aided by a knowledge of physical properties such as specific heats, infra-red and Raman spectra. Specific heat transitions, for example, may indicate the onset of molecular motion, which would give rise to a narrowing of the absorption spectrum. The converse is not necessarily true, however, since the absorption spectrum is only affected when the mean reorientation rate is of the same order of magnitude as the line-width. Thus changes in the line-width need not imply the existence of a specific heat anomaly.

Another important consideration is the purity of the samples. Both the second moment and relaxation time may be affected; e.g. an apparent narrowing of the anthracene spectrum was found to be due to the presence of an impurity (Rushworth 1952).

It was decided to measure the second moment and spin-lattice relaxation times for a sample of isopentane. Experiments made on straight-chain paraffins (Rushworth 1954 for example) have shown methyl group rotation occurring even at the lowest temperatures. It would be of interest, then, to examine the short, branched-chain molecule, isopentane, where the methyl groups are relatively close to one another. Rotation of all three methyl groups leads to a low theoretical second moment, and it might be expected that rotation of the branched-chain methyl group would be inhibited to some extent by the close proximity of its neighbouring methyl groups.

FIG. 8.

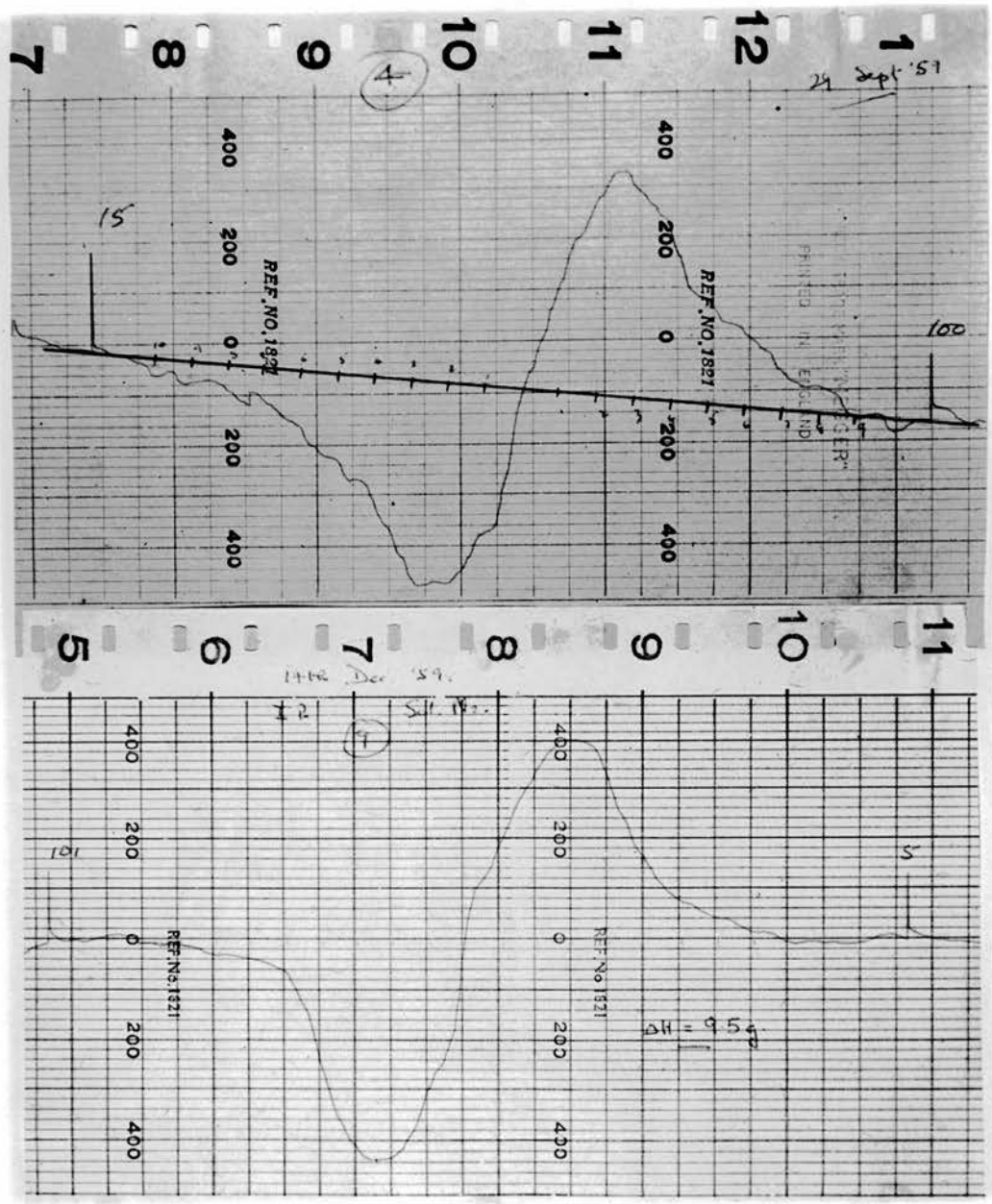
7
8
9
10
11
12
1
29 Sept '59
400
200
0
200
400
REF. NO. 1821
15
100
5
6
7
8
9
10
11
14th Dec '59.
101
5
REF. No 1821

FIG. 8.

Before commencing any new experimental work, however, it was necessary to resolve certain difficulties which had become apparent in the functioning of the apparatus. The apparatus was essentially that constructed by Andrew, Eades and Rushworth in 1950, and had been in use with only minor improvements for eight years. A decrease in the signal to noise ratio and general stability had reduced the sensitivity of the apparatus.

Another disturbing feature was that the output of the lock-in amplifier - the first derivative of the absorption line-shape - displayed a steadily increasing shift in zero when the line was being traced out (Fig. 8). The cause of this zero-shift was not obvious, and the remedy obscure. It was essential, however, for this to be removed, since the calculation of the second moment is greatly influenced by the wings of the absorption line (Andrew 1955) and the experimental results might then be rendered meaningless.

It was thought that modulation frequency pick-up might cause this zero-shift, and filters were designed following Robinson and Geiger (1958). Although the pick-up was reduced, the main fault remained.

The various power supplies were then checked, and, although some showed instability, there was no evidence to suggest the cause. New power supplies were installed as they became available.

The lock-in amplifier was itself unsatisfactory, since the output was unstable and showed a considerable zero-drift even with strong signals. Following the review article of Valley and Wallman, it was decided to construct an instrument based on the circuit of Cox (1953), described in section 3.2.

An alternative low-frequency generator was also constructed to give a modulation frequency of 285 c/s, since an increased modulation frequency would give a slightly higher signal to noise ratio as mentioned earlier.

These instruments were tested and found to perform satisfactorily, but, although the zero-drift was largely eliminated, the zero-shift remained.

The fault was eventually found to be due to the Kovar seal in the cryostat being slightly magnetic. This seal was situated between the magnet pole-pieces, and the sample was therefore being drawn bodily through the slightly inhomogeneous magnetic field as the field was being changed. When this seal was replaced the apparatus showed no zero-shift.

The original cryostat described by Lawrenson (1958), had itself been found unsatisfactory at temperatures between 40° and 60°K due to an excessive "cold-leak" to the specimen from the liquid hydrogen bath through the metal casing. A new cryostat was therefore designed, and has been described earlier.

The apparatus was then in a fit condition for experimental work to be undertaken, and Fig. 9 shows a typical absorption curve with the modified apparatus. There were, however, continual snags, breakdowns and instabilities, some of which were never completely resolved.

4.2 Experimental Results

The specimen of isopentane to be examined was obtained from the Chemical Research Laboratory, Teddington, and was quoted as having a mole per cent purity of 100%, determined from freezing-point measurements. This was vacuum distilled from the standard ampoule into several sample tubes of approximately 1 cc. volume specially made to fit the nuclear resonance coil.

4.2.1. Thermal Data

The specific heat (from 13°K) to the boiling point and the heat of fusion have been measured by Schumann, Aston and Sagenkahn (1942) and repeated by Guthrie and Huffman (1943). No specific heat transition was found between 13°K and the melting point, but both authors report a slight anomaly at 70°K, where there is a small bump on the specific heat curve. No possible explanation was given for this by those authors, but it was thought that the n.m.r. line-shape might also be affected by this peculiar anomaly.

The physical constants for isopentane were obtained from Timmermans (1950)

	Temperature	Heat of Melting
Freezing Point	-159.9°C	17 cal/gm.
Boiling Point	27.85°C	

4.2.2. Molecular and Crystal Structure

Neither the molecular nor the crystal structure for isopentane have been determined. Normal paraffin structures have been investigated by Müller (1928, 30, 32) using X-ray diffraction techniques. Using a single crystal, he found the exact structure of $C_{29}H_{60}$. The molecule is composed of plane, zig-zag chains of carbon atoms with tetrahedral angles between the C-C bonds whose length is 1.54 Å. The unit cell of the crystal lattice is orthorhombic, of dimensions a = 7.45 Å, b = 4.97 Å, c = 77.2 Å. The carbon chains are arranged along the c-axis of the unit cell.

For lower members of the paraffin series Müller found that the structures were similar to that of $C_{29}H_{60}$, with the a and b dimensions remaining the same, and the c dimension showing an increase of approximately 2.5 Å for each additional CH_2 group.

The application of Müller's results to the calculation of second moments of long-chain hydrocarbons has been discussed by Andrew (1950).

In the work reported here, the molecular constants are assumed similar to those of isobutane, and are quoted from "Interatomic

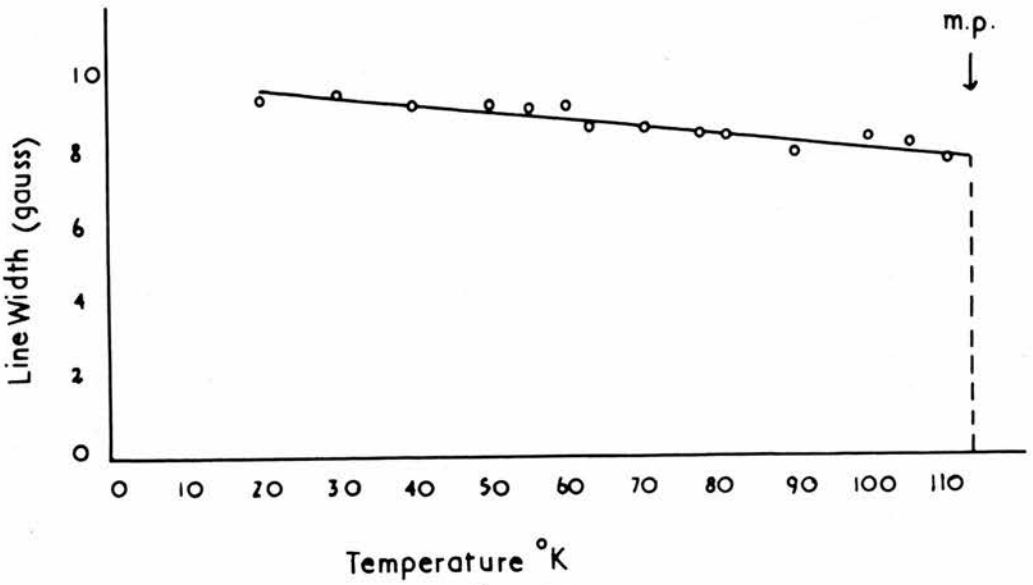
m.p.
Line Width (gauss)
0
2
4
6
8
10
0 10 20 30 40 50 60 70 80 90 100 110
Temperature °K

FIG. 10.

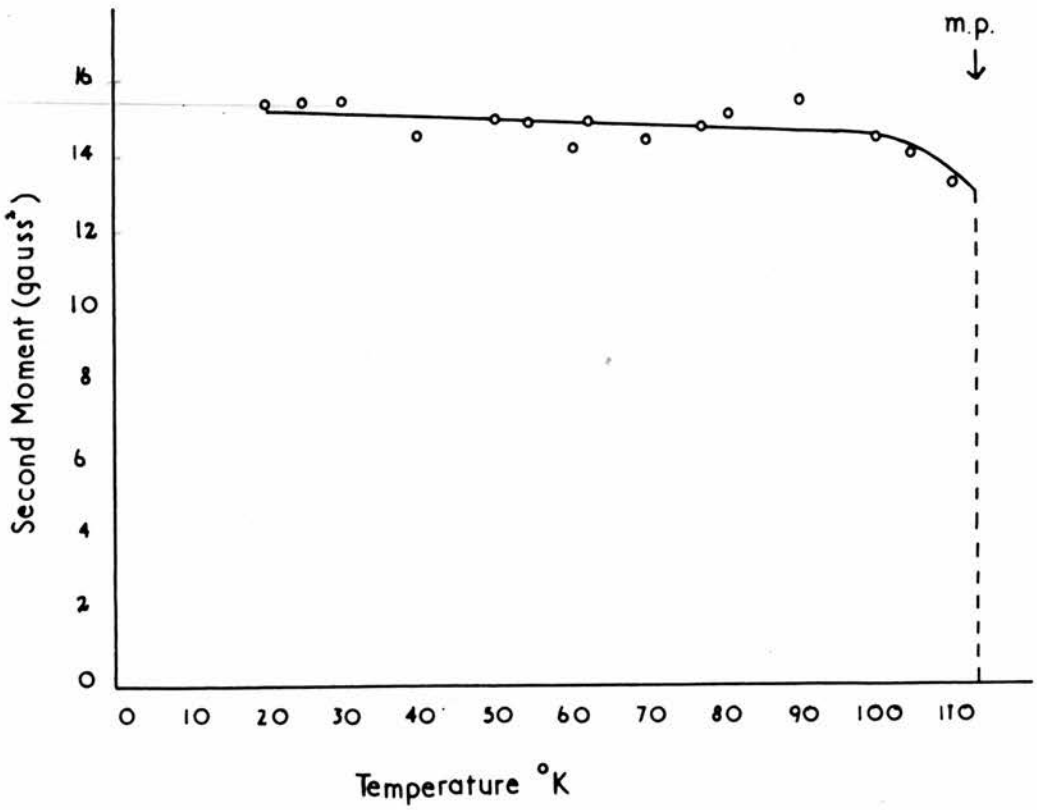
m.p.
Second Moment (gauss²)
0
2
4
6
8
10
12
14
16
0 10 20 30 40 50 60 70 80 90 100 110
Temperature °K

FIG. 11.

Distances" (1958).

C - C distance	1.54 ± 0.02 Å
C - H distance	1.09 Å
C - C - C angle	$111°30' \pm 2°$
H - C - H angle	$109°28'$

4.2.3 Absorption Spectrum

The line-widths and second moments of the resonance curves were determined from measurements of the recording meter traces. These traces give, in fact, the first derivative of the true absorption line, as has been shown earlier.

The line-widths, defined as the interval between positions of maximum and minimum slope, were measured in gauss from 20°K to the melting point, and are plotted against temperature in Fig. 10.

The second moments were calculated from the derivative curves in the manner of Pake and Purcell (1948), the trapezium rule being used to perform the numerical integration. A computer programme was devised for these calculations, and appears in the Appendix.

These experimental values for the second moment must be corrected for the broadening of the absorption line caused by the finite modulation of the magnetic field. It was shown by Andrew (1953) that if S_2' is the experimentally measured value of the second moment, the

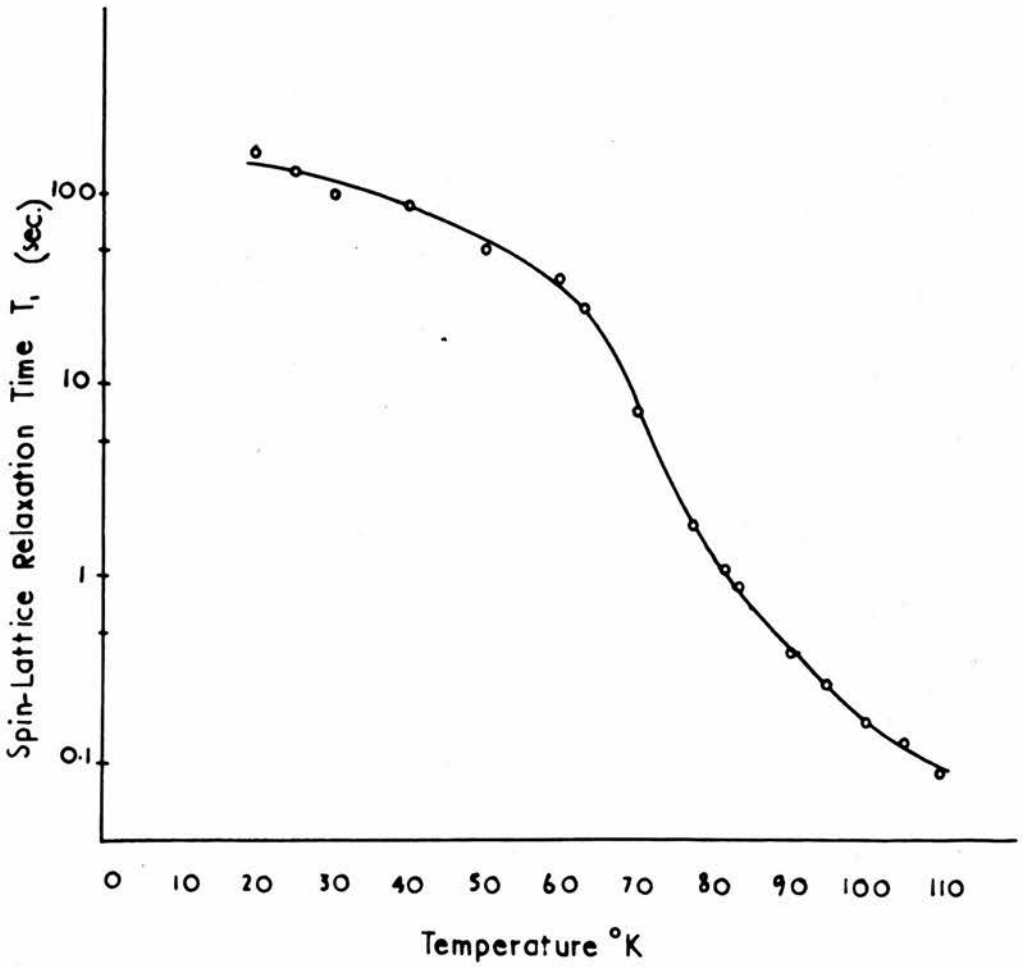
Spin-Lattice Relaxation Time T_1 (sec.)
100
10
1
0.1
0
10
20
30
40
50
60
70
80
90
100
110
Temperature °K

Fig. 12.

true value, S_2, for the second moment is given by

$$S_2 = S_2^1 + \frac{1}{4} hm^2$$

where hm is the modulation amplitude.

The variation with temperature of the second moment of isopentane is shown in Fig. 11. It will be seen that both the second moment and line-width values suffer no appreciable change from 20°K to the melting point, apart from the slight increase with decrease in temperature, attributable to thermal contraction of the lattice. The specific heat "bump" is not reflected in the n.m.r. line-shape measurements.

4.2.4. Spin-Lattice Relaxation Time Measurements

The spin-lattice relaxation time, T_1, was measured at temperatures between 20°K and the melting point. The experimental values are shown as a function of temperature in Fig. 12.

Two methods were used for the measurement of T_1, and have been described by Bloembergen, Purcell and Pound (1948). The actual method used depends on the value of T_1 itself, since this could be measured directly for times greater than about 30 seconds. This method consists of observation of the recovery of signal strength after the sample has been saturated, noting the gradual increase of the output meter reading. For times less than 30 seconds, the progressive saturation method is used, in which the signal strength is measured for gradually increasing radio-frequency fields. This method gives relative values of T_1, but these

are convertible to absolute values provided the direct method is used at a common temperature.

In the direct measurement of T_1, a high radio-frequency level is used in order to saturate the specimen. In equation 12 for the population ratio, the factor $\gamma^2 H_1^2 T_1 T_2$ becomes very much greater than unity, and the observed absorption intensity falls to zero. The radio-frequency level is then reduced by a factor of 100, and the subsequent regrowth of the signal observed on the recording meter. The slope of a plot of the meter reading against time on semi-log paper then gives the value of T_1 at the temperature measured. This process is repeated at other temperatures for which T_1 is greater than 30 seconds.

For lower values of T_1, the indirect, progressive saturation method is used. The basic assumption made here is that the intensity of absorption is proportional to the degree of saturation. This implies that, from equation 12, when $n/n_o = \frac{1}{2}$, or $\gamma^2 H_1^2 T_1 T_2 = 1$, the intensity of the absorption signal is halved. At temperatures denoted by A and B we should then have the relation between the relaxation times:

$$(H_1^2 T_1 T_2)_A = (H_1^2 T_1 T_2)_B \qquad (13)$$

where H_{1A} and H_{1B} are the radio-frequency amplitudes which reduce the observed signal to half of its maximum values at temperatures A and B

respectively. The ratio of the spin-spin relaxation times is obtained from the inverse ratio of the line-widths at the two temperatures, and H_1 is proportional to the measured output from the signal generator. Equation (13) may then be expressed

$$\frac{(T_1)_B}{(T_1)_A} = \frac{(V_A)^2}{(V_B)^2} \cdot \frac{\Delta H_B}{\Delta H_A} \qquad (14)$$

where V_A, V_B are the signal generator radio-frequency voltage levels corresponding to $(H_1)_A$, $(H_1)_B$. This method therefore gives relative values of T_1, and the proportionality factor is obtained by measurement of T_1 at a temperature where both methods can be used, in this case at 60°K where T_1 is found to be 39.7 seconds.

There are two aspects concerning the progressive saturation method which may affect the accuracy of the measurements (Andrew, 1955). First, the progressive saturation method applies only when $\omega\, mT_1 \ll 1$, or $\omega\, mT_1 \gg 1$, where $\omega\, m/2\pi$ is the modulation frequency. The latter condition is true for the values reported here. Secondly, this method assumes that the line-shape (linked with T_2) remains constant during saturation. This is not necessarily true, since the amount of saturation will vary with the position in the absorption line. A knowledge of the spin-spin relaxation time, T_2, is required in this method, and T_2 is directly related to the normalised line-shape. Changes in line-shape during saturation will then affect the result,

since T_2 is taken in these measurements to be proportional to the line-width in the unsaturated state.

4.3 Discussion of Results

4.3.1 Absorption Spectrum

The experimental value of the second moment of isopentane, taken as 15.0 ± 1 gauss^2 at 60°K, must be compared with the theoretical rigid-lattice value.

The calculation of the theoretical second moment may be split into two parts - the intramolecular contribution, due to neighbouring protons in the same molecule, and the intermolecular contribution from protons in neighbouring molecules. Knowledge of the molecular and crystal structures is therefore necessary for this calculation to be performed accurately.

The intramolecular contribution to the rigid-lattice second moment has been calculated using the projected molecular configuration detailed in Sect. 4.2.2, and following the theory outlined in Sect. 2.2. A computer programme was written for this calculation, and appears in the Appendix. The rigid lattice value found by this method was 25.2 gauss^2.

It is impossible to calculate exactly the intermolecular contribution to the second moment without a knowledge of the crystal structure. Andrew and Eades (1953a) made an estimate of the intermolecular contribution to the second moment of n-hexane and obtained a value of 9.6 gauss^2, with an uncertainty of 1.5 gauss^2.

This value has been used for other hydrocarbons where the degree of molecular packing is similar (Rushworth 1954, Lawrenson 1959, Hoch 1963). This similarity is shown by the approximate equality of lattice energies, a rough value of which is furnished by the sum of the heats of vaporisation, fusion and transition. Values for n-hexane and iso-pentane are 115 cal/gm. and 99 cal/gm. respectively (Timmermans 1950), indicating a slightly lower degree of packing in isopentane. It might then be expected that the intermolecular contribution to the second moment for isopentane will be of the same order as, but slightly less than that for n-hexane. Accordingly, the value for isopentane is taken as 9.6 gauss^2, with an increased uncertainty of $\pm$ 2 gauss^2.

The total theoretical rigid lattice second moment is thus taken as 34.8 $\pm$ 2 gauss^2, to be compared with the experimental value of 15 $\pm$ 1 gauss^2 at 60°K, a value which itself is less than the rigid lattice intramolecular second moment. This large discrepancy of 19.8 gauss^2 between theory and experiment implies that the molecules cannot be completely rigid in the lattice, and possible forms of molecular motions must now be considered. These motions may be:

(a) reorientation of the molecules about their long axes,

(b) reorientation of one or more of the methyl groups about their C-C axes.

The effect of rotation of the whole molecule on the intramolecular

contribution to the second moment can be calculated on the basis of the theory outlined in Sect. 2.2.

This contribution is reduced from 25.2 to 4.2 gauss^2, a reduction of 19.0 gauss^2 to which must be added the reduction in the intermolecular contribution. The total reduction would then give a very low value for the theoretical second moment, and such a mechanism is therefore considered unlikely. It might be considered, however, that only a fraction of the protons are rotating - for example, one half of the molecule rotating with respect to the other - in which case the average intramolecular contribution would be reduced by an amount less than 19 gauss^2. Although such a mechanism cannot be ruled out, it is considered unlikely in view of the results already obtained from other paraffins.

Rotation of the methyl groups about their end C-C axes must now be considered. For cyclohexane, Andrew and Eades (1953b) calculated the effect on the intermolecular contribution due to rotation of the molecules about their triad axes. This theory may be applied to determine the effects of rotation of the methyl groups on the intramolecular contribution here, and has been described in detail by Eades (1952).

The reductions in the intramolecular contribution to the second moment were calculated for combinations of the three methyl groups

rotating. The reductions found were:

(1) 11.7 gauss^2 for both end methyl groups rotating

(2) 6.4 gauss^2 for the side-chain methyl group rotating

(3) 15.9 gauss^2 for all three methyl groups rotating.

It would appear from these results that the most likely form of motion occurring in isopentane is the one in which all three methyl groups are rotating. The total reduction of 19.8 gauss^2 required to match theory with experiment, would then comprise the 15.9 gauss^2 reduction in the intramolecular contribution, and a reduction of 3.9 gauss^2 in the intermolecular contribution. This latter value seems reasonable in view of values already obtained for n-pentane, n-hexane and n-octane of 4.4, 3.7 and 4.8 gauss^2 respectively.

In the case of n-butane, however, Hoch (1963) has found the reduction in the intermolecular contribution to be 2.1 gauss^2. The equivalent reduction for isopentane (which may be considered to be the n-butane molecule in which a hydrogen in a methylene group has been replaced by a methyl group) would be expected to be greater, since nine out of the twelve protons in each molecule are moving.

The theoretical second moment for isopentane, when all three methyl groups are rotating, would then consist of an intramolecular contribution of 9.3 gauss^2, and an intermolecular contribution of 5.7 gauss^2. This gives a value of 15.0 gauss^2, agreeing with the

experimental value at 60°K, thus confirming that motion of the side-chain methyl group cannot be greatly hindered due to its position.

4.3.2 Relaxation Measurements

Spin-lattice relaxation time measurements yield further information about reorientation processes. Such reorientation is one of the most important relaxation mechanisms.

If the reorientation process can be described by a single correlation time, τ_c, it can be shown (Bloembergen, Purcell and Pound, 1948) that the relation between T_1 and τ_c is of the form

$$\frac{1}{T_1} = C\left[\frac{\tau_c}{1+\omega^2\tau_c^2} + \frac{4\tau_c}{1+4\omega^2\tau_c^2}\right] \qquad (15)$$

where $\omega/2\pi$ is the radio-frequency, and C is a constant. If the reorientation process is hindered by a potential barrier of height E per mole, the variation of τ_c with temperature should be of the form

$$\tau_c = \tau_o \exp(E/RT) \qquad (16)$$

where R is the gas constant per mole.

If, further, we consider only conditions where $\omega\tau_c \gg 1$, equation (15) simplifies to

$$T_1 = \frac{\omega^2\tau_c}{2C} \qquad (17)$$

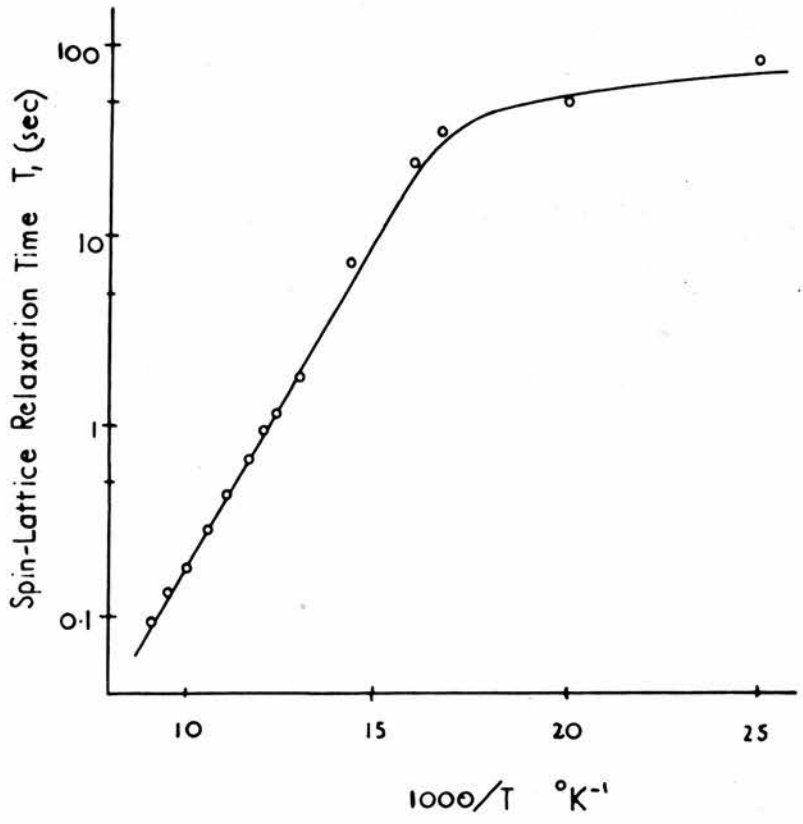
Spin-Lattice Relaxation Time T, (sec)
100
10
1
0·1
10
15
20
25
1000/T °K⁻¹

FIG. 13.

Substituting for τ_c from (14) then gives

$$T_1 = \frac{\omega^2 \tau_0}{2C} \exp\left(E/RT\right) \qquad (18)$$

or

$$\log T_1 = \log\left(\frac{\omega^2 \tau_0}{2C}\right) + \frac{E}{RT} \log e \qquad (19)$$

A plot of log T_1 against $1/T$ should then give a straight line whose slope gives E. For isopentane, a straight line is obtained for temperatures between 60°K and the melting point. This is shown in Fig. 13. A least squares calculation, for which a computer programme appears in the Appendix, gives the slope from which the barrier height, E, is found to be 1.92 k cal/mde.

Equation (15) has a minimum value for $\omega\tau_c = 0.62$, and the expression for T_1 then reduces to

$$(T_1)_{min} = \frac{0.31}{C} \qquad (20)$$

If a minimum is found in the T_1 vs temperature curve a value of C may be determined. Values of τ_c corresponding to the various T_1 values can then be obtained using equation (17). A graph of log against $1/T$ should then give a straight line, and a value of E may then be calculated. This method is not strictly applicable to the experimental results quoted here, since an extrapolation would be necessary to give the minimum T_1 value.

The relative lack of variation of T_1 below 60°K is explained from another viewpoint. A consideration of the small mass of the proton, and the relatively low potential barriers to rotation led Powles and Gutowsky (1955) to propose that the methyl groups reorient more by quantum mechanical tunnelling through the barrier than by classical rotation over the barrier.

The theory of Bloembergen, Purcell and Pound (1948), modified by Solomon (1955), is used to calculate the proton spin-lattice relaxation time for methyl groups undergoing hindered rotations and molecular tumbling motions in solids, assuming Debye spectral density functions for both motions. It is assumed also that there is no interaction between neighbouring methyl groups, and that the barrier to rotation is sinusoidal and time independent.

In the case of methyl group reorientation and molecular tumbling, considering dipolar interactions only within a given methyl group, the modified version of equation 15 is written (Stejskal & Gutowsky, 1958):

$$\frac{1}{T_1} = \left[\frac{3\gamma^4\hbar^2}{40 r_o^6}\right]\left[\frac{4\tau_{c1}}{1+\omega_o^2\tau_{c1}^2} + \frac{16\tau_{c1}}{1+4\omega_o^2\tau_{c1}^2} + \frac{3\tau_{c2}}{1+\omega_o^2\tau_{c2}^2} + \frac{12\tau_{c2}}{1+4\omega_o^2\tau_{c2}^2}\right] \qquad (21)$$

where r_o is the H-H distance, τ_{c1} is the correlation time for the

molecular tumbling, τ_c is the correlation time for methyl group reorientation, given in terms of the tunnelling frequency, ν_t, as (Powles & Gutowsky, 1953)

$$\tau_c = {}^1/_{3\pi\nu_t} \qquad (22)$$

and

$$\tau_{c2}^{-1} = \left[{}^1/_{\tau_c} + {}^1/_{\tau_{c1}} \right] \qquad (23)$$

If methyl group reorientations are important only, τ_{c1} is set equal to infinity, and equation (21) reduces to an expression for T_1 having a single minimum, for which value $\omega\tau_c = 0.61$.

If, further, we consider only conditions where $\omega\tau_c \gg 1$, equation (21) reduces to

$$\frac{1}{T_1} = \frac{9\gamma^4\hbar^2}{40 r_o^6} \cdot \frac{2}{\omega_o^2 \tau_c} \qquad (24)$$

Combining equations (22) and (24), we then have the expression for the tunnelling frequency in terms of T_1:

$$= \frac{20}{9\pi} \cdot \frac{\omega_o^2 r_o^6}{\gamma^4 \hbar^2} \cdot \frac{1}{T_1} \qquad (25)$$

Stejskal and Gutowsky also calculated the variation in the tunnelling frequency with temperature for various values of barrier height. A plot of log ν_t against ${}^{1000}/T$ yields a regular family of curves, whose slopes and infinite temperature limits agree with

classical theory in the higher temperature region. At lower temperatures, however, there is a discrepancy between classical and quantum-mechanical predictions, as the lines curve, ν_t decreasing asymptotically towards the limiting value of the ground torsional state.

Stejskal, Woessner, Farrer and Gutowsky (1959) applied the tunnelling theory to measurements of line-widths and spin-lattice relaxation times for several compounds containing reorienting methyl groups. Although a considerable agreement was found with the tunnelling theory for several compounds studied, this was not the case for neopentane, the more compact isomer of isopentane. Here the basic assumptions that the potential barrier to rotation is sinusoidal and time independent cannot be valid, since the interproton distances within a given methyl group are comparable with those between neighbouring methyl groups (1.77(89) Å and a maximum of 1.88(763) Å respectively, for isopentane). There will therefore be a great deal of interaction between neighbouring methyl groups here.

An application of the tunnelling theory to the measurements of spin-lattice relaxation times for isopentane leads to an apparent barrier height of 3.65 Kcal in the temperature region above 60°K, and 4.9 Kcal below 60°K.

The value of 3.65 Kcal must be compared with the value for the barrier height of 1.92 Kcal obtained from the classical activation

energy calculation. As has been pointed out earlier, the tunnelling theory cannot be expected to be valid where there is interaction between neighbouring methyl groups, as there is in neopentane. It would be reasonable to assume here that the interlocking, or "cog-wheeling" of neighbouring methyl groups would lead to a lowering of the effective barrier height predicted by the tunnelling theory, and that the value predicted by the classical calculation is to be preferred for such motions. In their paper, Stejskal et al stated that "the situation here is sufficiently complex that it would perhaps be better to stop with the classical activation energy, and let well enough alone", whilst referring to neopentane.

At low temperatures, however, the cog-wheeling mechanism may not predominate and the methyl groups might then act as if they were effectively independent. Tunnelling theory would then be more physically realistic, and the value of 4.9 Kcal obtained would represent the real barrier to the motion of a methyl group in isopentane. This value agrees with the general range of barrier heights predicted by the tunnelling theory, 5 to 6 Kcal, quoted by Powles and Gutowsky (1955).

Hoch (1963) has applied tunnelling theory to the relaxation time results obtained for n-butane. The values obtained are very similar to those of isopentane, as is the disagreement with classical theory. The short distances between methyl groups here may lead to a form of

cog-wheeling as suggested for isopentane.

The results for n-butane and isopentane show that further work is required to investigate the effects of the interactions which must occur between neighbouring methyl groups in such short, tightly packed molecules. The separation of the methyl groups in a molecule of n-butane is less than 5 Å and the closest approach between neighbouring methyl groups in a crystal of n-pentane has been estimated as 0.53 Å, based on the X-ray work of Müller (Rushworth, 1954). This low value is inconsistent with the value of the van der Waals radius for the methyl group, and Müller has suggested ways by which this distance could be eased.

It would also be of interest if low temperature X-ray studies of these and similar hydrocarbons were made to give a clearer picture of their crystal structure. This would enable more accurate calculations to be made for the intermolecular second moment, and also throw more light on the reorientation processes which occur.

More information is gained from line-width measurements when transitions are observed. The second moment of isopentane is much less than the rigid lattice value even at 20°K, and it would be necessary to extend these measurements to liquid helium temperatures to investigate whether the line broadens, or methyl group reorientation is still evident at these low temperatures.

5. SUMMARY

5. Summary.

The existing apparatus has been overhauled and modified, new equipment being introduced as it became available. In an effort to eliminate the major fault in the apparatus, the zero shift in the lock-in amplifier output, a new lock-in amplifier and audio-frequency generator were constructed. The fault was eventually traced to a magnetic component in the existing cryostat. The cryostat was considered unsuitable for measurements at temperatures below 40°K, and consequently a cryostat in which these faults were eliminated was designed. This was found to give good results even at the lowest temperatures.

The nuclear magnetic resonance absorption spectrum and spin-lattice relaxation times for isopentane have been studied at temperatures from 20°K to the melting point.

Second moment measurements indicate reorientation of the three methyl groups about their C-C axes, even at 20°K. Spin-lattice relaxation time measurements were used to determine approximate values for the barriers restricting reorientation, applying both classical and tunnelling theories. Discrepancies with theory are discussed.

In conclusion, the author would like to express sincere thanks to Dr. F.A. Bushworth for his guidance and encouragement during the course of this work; to Professor J.F. Allen, F.R.S. for his interest and advice on the construction of the cryostat, to Mr. J. Gerrard for his

assistance with the photography and supplies of components and materials, and to the technical staff for their help and co-operation at all times.

6. APPENDIX - COMPUTER PROGRAMMES

```
Jv1
TEXT
SECOND MOMENT
1)v1=TAPE*
n1=no/2
v51=0
v53=0
2)v50=vno×vn1
v51=v51+v50
v52=vn1×vn1
v52=v52×v50
v53=v53+v52
no=no-1
n1=n1-1
→2,n1≠0
v53=v53/v51
PRINTv53,3043
→1
(→0)
**************
```

Fig. 14.

6. Appendix - Computer Programmes.

6.1 Introduction.

Many of the calculations necessary in this research programme are simple, in essence, but require to be repeated many times. These, and other more complex problems were solved by the Ferranti Sirius Computer at the Heriot-Watt College, Edinburgh.

Sirius is a small decimal computer. In its basic form it has a store of twenty nickel delay lines, each of which consists of fifty locations. It therefore has a total capacity of one thousand locations. Each computer location holds ten decimal digits. These digits represent either a number or a computer instruction. Information is fed into the computer and extracted from it by means of a five-channel punched paper tape.

The basic frequency of the machine is $\frac{1}{2}$ Mc/s, with a word-time of 80 μs.

The computer programmes listed here are written in the Autocode language of the Sirius, but these may be converted without difficulty into the code of another computer. Reference need only be made to the corresponding coding manuals (Ferranti 1962).

6.2 Experimental Second Moment.

In section 2.2 it was shown that the second moment is given by

```
Jv1
1)v1=TAPE*
n1=no/2
v102=0
v104=0
v106=0
2)v100=vn1-v1
v101=vno
v102=v102+v101
v103=v101Xv100
v104=v104+v103
v105=v103Xv100
v106=v106+v105
no=no-1
n1=n1-1
→2,n1≠0
v104=v104/v102
v104=v104+v1
PRINTv104,3063
v106=v106/v102
v107=v104-v1
v107=v107Xv107
v106=v106-v107
v106=SQRTv106
PRINTv106,3063
v106=v106/v104
v106=v106X100
PRINTv106,3063
→1
(→0)
```

Fig. 15.

the expression

$$\langle (\Delta H)^2 \rangle_{av} = \frac{1}{3} \frac{\int h^3 \frac{d f(h)}{dh} dh}{\int h \frac{d f(h)}{dh} dh} \qquad (7)$$

The quantity $d f(h)/dh = F(h)$ is precisely the reading of the output meter, in arbitrary units. The integrals are evaluated directly using the trapezium rule:

$$\text{Second Moment} = \frac{1}{3} \frac{\sum h^3 F(h)}{\sum h F(h)}$$

The programme (Fig. 14) prints out this result for the second moment using the data taken from experimental curves.

Data is read in as the values $h_1 \ldots\ldots h_n$, followed by the corresponding values $F(h_1) \ldots\ldots F(hn)$, both sets in arbitrary units. The result is converted to units of gauss^2 using the calibration pips on the experimental curve and the field sweep calibration.

The modulation correction outlined in Sec. 4.2.3 is then applied to give the corrected value for the second moment.

6.3 Standard Deviation.

The mean value, standard deviation, and coefficient of variation (Topping) of a set of results may be obtained from this programme (Fig. 15).

Data is read in as the values of the quantity $x_1 \ldots\ldots x_n$, taken in any order, followed by the frequency of occurrence, $f_1 \ldots\ldots f_n$, in

```
Jv1
4)v1=TAPE*
n1=no/2
n4=no
n2=n1
v109=n1
v101=0
v103=0
v104=0
v106=0
1)v100=vn2
v101=v101+v100
v102=v100xv100
v103=v103+v102
n2=n2-1
→1,n2≠0
v101=v101/v109
PRINTv101,3063
*2)v104=v104+vn4
n4=n4-1
→2,n4≠n1
v104=v104/v109
PRINTv104,3063
3)v105=vnoxvn1
v106=v106+v105
no=no-1
n1=n1-1
→3,n1≠0
v107=v101xv104
v107=v107xv109
v108=v101xv101
v108=v108xv109
v106=v106-v107
v103=v103-v108
v106=v106/v103
PRINTv106,3063
→4
(→0)
**********************************************
```

Fig. 16.

the corresponding order.

This programme was used to give the mean values for all the results quoted in this thesis.

6.4 Gradient by Least Squares.

The best straight line through a set of points is determined by this programme.

For the simple case where the relation between x and y is assumed linear, and the values of x are accurately known, it is found that (Braddick):

(a) The best straight line passes through the centre of gravity of the N points, i.e. through the point whose coordinates are

$$\bar{x} = \frac{\Sigma x_n}{N} \qquad \bar{y} = \frac{\Sigma y_n}{N}$$

(b) The best slope is given by

$$m = \frac{\Sigma x_n y_n - N \bar{x} \bar{y}}{\Sigma x_n^2 - N \bar{x}^2}$$

This programme (Fig. 16) prints out in order $\bar{x}$, $\bar{y}$ and m. Data is read in as $x_1 \ldots\ldots x_n$, followed by the corresponding values $y_1 \ldots\ldots y_n$.

```
Jv1
TEXT
INTER-PROTON DISTANCES--ISOPENTANE---SECOND MOMENT
v10=TAPE*
n0=10
v6=0
2)n1=3
1)n2=n0+n1
v1=vn0-vn2
v2=v(1+n0)-v(1+n2)
v3=v(2+n0)-v(2+n2)
v1=v1Xv1
v2=v2Xv2
v3=v3Xv3
v4=v1+v2
v4=v4+v3
v4=SQRTv4
PRINTv4,3025
v4=v4Xv4
v5=v4Xv4
v5=v4Xv5
v5=1/v5
v6=v6+v5
n1=n1+3
→1,n2≠43
n0=n0+3
→2,n0≠43
PRINTv6,3006
v7=715.9
v7=v7/12
v6=v6Xv7
TEXT
S=
PRINTv6,4043
STOP
****(→0)
**********
```

Fig. 17.

6.5 Intramolecular Second Moment.

It has been shown in Sect. 2.2 that the Van Vleck formula for the rigid lattice intramolecular second moment reduces to

$$S = \frac{715.9}{Nr} \sum_{jk} r_{jk}^{-6} \qquad (9)$$

This programme (Fig. 17) prints out, in order, the inter-proton distances in Angstrom units, the sum of the inverse sixth power of these distances, and the value of S given by equation (9), for isopentane.

Data is read in as the coordinates $(x_1, y_1, z_1 \ldots x_{12}, y_{12}, z_{12})$ of the protons, taken in order.

Fig. 18 shows these results for isopentane.

Fig. 18.

```
CLEARED STORE.

INTER-PROTON DISTANCES--ISOPENTANE---SECOND MOMENT

 1.77980
 1.77984
 2.48866
 2.48865
 3.79296
 5.56364
 4.82881
 4.82863
 3.53723
 4.96210
 4.12165
 1.77984
 3.05960
 2.48865
 3.14835
 4.82858
 4.69155
 4.34065
 1.88763
 3.53682
 2.83534
 2.48865
 3.05963
 2.59686
 4.82825
 4.34067
 4.69134
 2.83507
 4.12091
 3.95999
 1.77984
 2.48171
 3.73632
 2.51465
 3.08063
 3.73666
 4.29290
 3.73664
 3.05408
 3.73676
 3.08104
 2.51456
 3.08030
 3.73582
 2.51400
 2.39753
 2.39787
 2.98630
 2.53977
 2.48093
 3.05408
 1.77890
 1.77965
 3.73755
 2.51465
 3.08115
 1.78010
 4.29453
 3.73632
 3.73728
 3.73729
 3.08000
 2.51456
 1.77944
 1.77990
 1.77939
 0.423147
S=
```

7. REFERENCES

REFERENCES

Anderson, H.L. (1949) Phys. Rev. 76, 1460.

Andrew, E.R. (1950) J. Chem. Phys. 18, 607.

Andrew, E.R. (1953) Phys. Rev. 91, 425.

Andrew, E.R. (1955) Nuclear Magnetic Resonance, Cambridge University Press.

Andrew, E.R. and Bersohn, R. (1950) J. Chem. Phys. 18, 159.

Andrew, E.R. and Eades, R.G. (1953a) Proc. Roy. Soc. A216, 398.

Andrew, E.R. and Eades, R.G. (1953b) Proc. Roy. Soc. A218, 537.

Andrew, E.R. and Finch, N.D. (1957) Proc. Phys. Soc. 70, 980.

Andrew, E.R. and Pushworth, F.A. (1952) Proc. Phys. Soc. B65, 801.

Bearden, J.A. and Watts, H.M. (1951) Phys. Rev. 81, 73.

Bloch, F., Hansen, W.W. and Packard, M.E. (1946) Phys. Rev. 69, 127.

Bloembergen, N. (1948) Nuclear Magnetic Relaxation. M. Nijoff, The Hague.

Bloembergen, N. (1949) Physica 15, 386.

Bloembergen, N., Purcell, E.M. and Pound, R.V. (1948) Phys. Rev. 73, 679.

Braddick, H.J.J. Physics of Experimental Methods. Chapman and Hall.

Cox, H.L. (1953) Rev. Sci. Inst. 24, 307.

Das, T.P. (1956) J. Chem. Phys. 25, 896.

Das, T.P. (1957) J. Chem. Phys. 27, 763.

Dicke, R.H. (1946) Rev. Sci. Inst. 17, 268.

Eades, R.G. (1952) Thesis, St. Andrews University.

Ferranti (1962). Ferranti Sirius Computer - Description of the Autocode.

Gorter, C.J. (1936) Physica 3, 995.

Gorter, C.J. (1951) Physica 17, 169.

Gorter, C.J. and Broer, L.F.J. (1942) Physica 9, 591.

Guthrie, G.B. and Huffman, H.M. (1943) J. Am. Chem. Soc. 65,1139.

Gutowsky, H.S. and Pake, G.E. (1950) J. Chem. Phys. 18, 162.

Hoch, M.J.R. (1963) Thesis, St. Andrews University.

Interatomic Distances (1958) Chemical Society Publication.

Lawrenson, I.J. (1958) Thesis, St. Andrews University.

Lawrenson, I.J. andRushworth, F.A. (1959) Arch. Sci. 12, Spec No., 116.

Müller, A., (1928) Proc. Roy. Soc. A120, 437.

Müller, A., (1930) Proc. Roy. Soc. A127, 417.

Müller, A., (1932) Proc. Roy. Soc. A138, 514.

Pake, G.E. (1948) J. Chem. Phys. 16, 327.

Pake, G.E. and Purcell, E.M. (1948) Phys. Rev. 74, 1184.

Pauli, W. (1924) Naturwissenschaften 12, 741.

Powles, J.G. and Gutowsky, H.S. (1953) J. Chem. Phys. 21, 1695, 1704.

Powles, J.G. and Gutowsky, H.S. (1955) J. Chem. Phys. 23, 1692.

Pound, R.V. and Knight, W.D. (1950) Rev. Sci. Inst. 21, 219.

Purcell, E.M., Torrey, H.C. and Pound, R.V. (1946) Phys. Rev., 69, 37.

Rabi, I.I., Millman, S., Kusch, P. and Zacharias, J.R. (1939), Phys. Rev. 55, 526.

Robinson, G.B. and Geiger, F.E. (1958) Rev. Sci. Inst. 29, 730.

Rollin, B.V. and Hatton J. (1948) Phys. Rev. 74, 346.

Rushworth, F.A. (1952) J. Chem. Phys. 20, 920.

Rushworth, F.A. (1953) Thesis, St. Andrews University.

Rushworth, F.A. (1954) Proc. Roy. Soc. A222, 526.

Schumann, S.C., Aston, J.G., Sagenkahn, M. (1942) J. Am. Chem. Soc. 64, 1039.

Solomon, I. (1955) Phys. Rev. 99, 559.

Stejskal, E.O. and Gutowsky, H.S. (1958) J. Chem. Phys. 28, 388.

Stejskal, E.O., Woessner, D.E., Farrar, T.C. and Gutowsky, H.S. (1959) J. Chem. Phys. 31, 55.

Timmermans, J. (1950) Physico-Chemical Constants of Pure Organic Compounds. Elsevier : Amsterdam.

Topping, J. Errors of Observation and Their Treatment. Institute of Physics.

Valley, G.E. and Wallman, H. Vacuum Tube Amplifiers. M.I.T. Radiation Laboratory Series, Vol. 18.

Van Vleck, J.H. (1948) Phys. Rev. 74, 1168.